MICROCOPY RESOLUTION TEST CHART
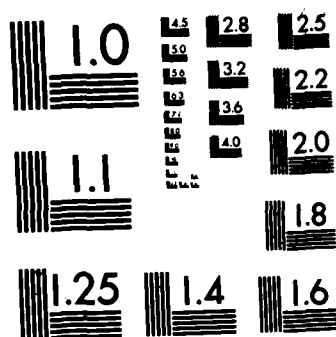NATIONAL BUREAU OF STANDARDS-1963-A

CRREL

REPORT 83-8

**US Army Corps
of Engineers**
Cold Regions Research &
Engineering Laboratory

Properties of urea-doped ice
in the CRREL test basin

ADA 128219

DTIC FILE COPY

DTIC
S ELECTE D
MAY 17 1983
B

83   05   17   028

For conversion of SI metric units to U.S./ British customary units of measurement consult ASTM Standard E380, Metric Practice Guide, published by the American Society for Testing and Materials, 1916 Race St., Philadelphia, Pa. 19103.

CRREL Report 83-8

March 1983

Properties of urea-doped ice in the CRREL test basin

Ken-ichi Hirayama

REPORT DOCUMENTATION PAGE		READ INSTRUCTIONS BEFORE COMPLETING FORM
1. REPORT NUMBER CRREL Report 83-8	2. GOVT ACCESSION NO. AD-A128 219	3. RECIPIENT'S CATALOG NUMBER
4. TITLE *(and Subtitle)* PROPERTIES OF UREA-DOPED ICE IN THE CRREL TEST BASIN		5. TYPE OF REPORT & PERIOD COVERED
		6. PERFORMING ORG. REPORT NUMBER
7. AUTHOR*(s)* Ken-ichi Hirayama		8. CONTRACT OR GRANT NUMBER*(s)* USAED, New England 82-C-0004
9. PERFORMING ORGANIZATION NAME AND ADDRESS U.S. Army Cold Regions Research and Engineering Laboratory Hanover, New Hampshire 03755		10. PROGRAM ELEMENT, PROJECT, TASK AREA & WORK UNIT NUMBERS CWIS 31355
11. CONTROLLING OFFICE NAME AND ADDRESS U.S. Army Engineer Division, New England 424 Trapelo Rd. Waltham, Massachusetts		12. REPORT DATE March 1983
		13. NUMBER OF PAGES 53
14. MONITORING AGENCY NAME & ADDRESS*(if different from Controlling Office)*		15. SECURITY CLASS. *(of this report)* Unclassified
		15a. DECLASSIFICATION/DOWNGRADING SCHEDULE

16. DISTRIBUTION STATEMENT *(of this Report)*

Approved for public release; distribution unlimited.

17. DISTRIBUTION STATEMENT *(of the abstract entered in Block 20, if different from Report)*

18. SUPPLEMENTARY NOTES

19. KEY WORDS *(Continue on reverse side if necessary and identify by block number)*
Hydraulic models
Ice
Model basins
Models
Model tests

20. ABSTRACT *(Continue on reverse side if necessary and identify by block number)*

In the course of model tests with urea-doped ice in the CRREL Ice Engineering Facility test basin, the growth process and the physical and mechanical properties of the model ice were investigated. The parameters which were varied were: urea concentration in the tank water, air temperature during growth, growth duration, and tempering time.

Uniformity of ice thickness and ice mechanical properties over the whole tank area were found to be satisfactory. The structure of the urea-doped ice was found to be similar to that of the ice except for a relatively thick incubation layer over a dendritic bottom layer.

Empirical relationships were established between: ice thickness and negative degree-hours; mechanical properties and growth temperature, urea concentration, and ice thickness; and reduction in mechanical properties and tempering time.

DD FORM 1473 EDITION OF 1 NOV 65 IS OBSOLETE

20. Abstract (cont'd).

The results of the study are presented in charts which permit reliable scheduling of model tests with required ice thickness and ice flexural strength.

PREFACE

Accession For

NTIS GRA&I ✓
DTIC TB ☐
Unannounced ☐
Just

By
Distribution/
Availability Codes

Dist | Avail and/or Special

A

iii

CONTENTS

ILLUSTRATIONS

Figure

TABLES

NOMENCLATURE

a	ratio of top layer thickness to total ice thickness
B	width of cantilever beam
b	ratio E_1/E_2
c	concentration of urea solution
c_0	initial concentration of urea solution
D	diffusion coefficient
E	elastic modulus obtained by downward loading
E'	elastic modulus obtained by upward loading
E_i	elastic modulus of ice at start of warm-up period
E_0	nominal elastic modulus of two-layer model
E_1	elastic modulus of top layer in two-layer model
E_2	elastic modulus of bottom layer in two-layer model
G	temperature gradient at the freezing interface
H	thickness of cantilever beam
h	ice thickness (average at six monitoring points)
h_c	ice thickness in testing area of tank
h_f	final ice thickness
h_i	ice thickness at start of warm-up period
h_t	thickness of top ice layer
Δh	$h - h_i$
h_{ia}	heat transfer coefficient between ice and air
I	moment of inertia about neutral axis of homogeneous beam
I_1	moment of inertia of top layer about neutral axis of two-layer model
I_2	moment of inertia of bottom layer about neutral axis of two-layer model
K	thermal diffusivity of ice
k	equilibrium partition coefficient of the solute
k_i	thermal conductivity of ice
L	beam length
ℓ	ice characteristic length
m	liquidus slope
P	load
p	arbitrary constant
q	arbitrary constant
r	radius of loading zone in modulus test
R	growth rate
T_a	ambient air temperature
T_{ai}	temperature at ice/air interface
T_{iw}	freezing temperature of the solution
t	time
v	coefficient of variation
z	distance from neutral axis
z_0	location of neutral axis of two-layer material
α	ratio r/L
δ	deflection
ϵ_t	strain at top of ice
γ_w	specific weight of water
σ	flexural strength obtained by downward loading
σ'	flexural strength obtained by upward loading
σ_i	flexural strength at start of warm-up period

σ_0	nominal strength of two-layer model
σ_t	stress at top surface of two-layer model
σ_1	tensile strength of top layer
σ_2	tensile strength of bottom layer
ϕ_{ia}	heat flux at ice/air interface
ϕ_i	heat flux through ice sheet
ρ_i	density of ice
λ	latent heat of fusion of ice
υ	Poisson's ratio
$\sum$	sum of degree-hours

PROPERTIES OF UREA-DOPED ICE IN THE CRREL TEST BASIN

Ken-ichi Hirayama

INTRODUCTION

Design of hydraulic structures to be erected in regions with severe winters must take into consideration potentially large ice forces. Examination of past records of measured ice thrusts on similar structures, and structural failure due to ice, is one way to estimate the ice forces to be expected. However, model studies are often required when new designs are being considered or when the influence of various parameters (structure geometry, ice characteristics, etc.) on ice–structure interaction is being investigated systematically. Such model studies and their qualitative as well as quantitative results can lead to better understanding of ice effects on structures. It is important that the model studies be complemented by field measurements and observation once a particular structure has been built, to verify model predictions and improve modeling techniques.

Simple dimensional analysis shows that physical modeling of ice–structure interaction where ice fails in bending requires that both the flexural strength σ and the elastic modulus E of ice be scaled in the same ratio as the geometric characteristic length. Therefore the ratio E/σ must be the same for the model ice and the prototype ice. However, mathematical analysis of ice forces on two-dimensional structures has shown that, under certain circumstances which often prevail in nature, the peak force exerted by the ice is independent of E (see, e.g., Yean et al. 1981), and formulas derived by Ralston (1977), Danys and Bercha (1976) and Nevel (1977) do not include E directly. On the other hand, that part of the total resistance of an icebreaker which is due to actually breaking the ice has been shown to be, in its dimensionless form, proportional to E/σ (Enkvist

1972). Some mo٤ ⋅ ⋅us attempt to correct model results for differences in E/σ between model ice and real ice when the former falls below about 1500. Values of model ice E/σ larger than 1500 ensure that the size of the broken floes is adequately modeled. The size of broken floes is directly related to ℓ, the ice characteristic length, which is proportional to the fourth root of E, so that a 100% error in E leads to only a 20% error in ℓ. Another argument which may be advanced for relaxing the theoretical requirement of keeping the ratio E/σ the same for the model and the prototype is that the icebreaking component of the total resistance is usually relatively small. Nevertheless, values of E for the model ice should remain sufficiently high to avoid excessive plastic deformation of the ice and consequently unrealistically high ice forces on structures.

Test basins without refrigeration capability use artificial model ice manufactured from various mixes of wax, plastic beads and other materials. Except for that proposed by Tryde (1977), the exact composition of most artificial ice is proprietary and not readily available. Until recently, refrigerated test basins grew their model ice from a saline solution. However, this has restricted model testing to scales no smaller than 1/20 because low-strength saline ice becomes plastic. Furthermore, saline ice leads to serious corrosion problems in equipment and instrumentation, and correspondingly expensive maintenance and/or protective measures. Timco (1979, 1980, 1981) proposed that model ice be grown from an aqueous solution of urea. His initial studies showed that such model ice could be used in studies with a geometric scale ratio down to 1/40. One advantage of urea-doped ice is the near elimination of corrosion problems in the test facility.

Urea-doped ice has been used as model ice in the test basin at the Ice Engineering Facility of the U.S. Army Cold Regions Research and Engineering Laboratory (CRREL) since 1980. This report presents the results of a systematic study of the properties of urea-doped ice based on measurements on about 50 ice sheets. The influence of urea concentration, ice thickness, and warm-up time (as explained in the following section) on the mechanical properties of the model ice was investigated. In particular, four urea concentrations in the test basin were studied. Prior to August 1981 the urea concentration by weight in the test basin water was 1.05%. In August 1981 the basin was emptied for clean-up and maintenance, after which three urea concentrations were successively used, namely 0.45%, 0.70% and 0.95%. The 0.95% concentration was selected for permanent use in the basin. The study resulted in a consistent method of growth of an ice sheet to achieve any required ice thickness from about 2 to 8 cm, with bending strength as low as about 15 kPa. Besides ensuring reliable and reproducible ice characteristics, this method allows better scheduling of test programs. The particulars of the method described in this report are valid only for the CRREL test basin, since they depend upon the specific refrigeration characteristics of the facility and the urea concentration used. However, similar methods can be devised for any ice testing facility.

EXPERIMENTAL FACILITY AND PROCEDURES

Ice test basin
The CRREL test basin has a useful length of 34.4 m (113 ft), a width of 9 m (30 ft), and a water depth of 2.4 m (8 ft). A 5.4 m (18 ft) long, 3 m (10 ft) wide, 2.4 m (8 ft) deep preparation tank is located at the east end of the main basin. Melting and recirculation tanks are located at the west end. The whole test basin is housed in an insulated, refrigerated room. The prep-tank area can be isolated from the main basin by a vertically sliding insulated door. The ceiling of the refrigerated room is 7.2 m (24 ft) above the maximum water level in the tank.

Room refrigeration is provided by seven forced air heat exchangers suspended from the ceiling at a height of 5.2 m (17 ft) above maximum water level; the total refrigeration capacity is 80 kW (2.8×10^5 Btu/hr), and the minimum air temperature which can be achieved is approximately $-23°C$ ($-10°F$). The refrigeration fluid is ammonia.

Ice growth procedure
Ice sheets are grown on the tank surface from an

aqueous solution of urea. The water is cooled primarily by heat exchange at the air/water interface. However, for water temperature above approximately $2°C$ ($35°F$), additional cooling is provided by pipes carrying ammonia located in a trench along the east end of the tank. At water temperature below $2°C$, these cooling pipes become fully encased in ice and are ineffective. Uniformity of water temperature in the tank, essential for achieving an ice sheet of uniform thickness and mechanical properties, is ensured by continuously circulating the water longitudinally with pumps and by vertically mixing it with air bubbler lines laid on the bottom of the tank. During the study, the water temperature was monitored regularly at six locations along the tank perimeter by a thermistor with a $1/50°C$ resolution.

When the water temperature is within $0.2°C$ of the freezing point of the urea solution, the circulation pumps and air bubblers are deactivated. Once the water surface is sufficiently calm, the ice sheet is initiated through wet seeding by spraying a fine mist of water in the air, which is kept at a temperature of about $-10°C$ ($15°F$). The fine mist turns into ice crystals which settle on the water surface where they initiate the ice sheet. Wet seeding is necessary to ensure uniform crystal size in the ice sheet (and therefore uniformity of mechanical properties) and a sufficiently high ratio of ice thickness *to crystal size. The crystal size of an ice sheet grown in this manner is typically of the order of 2 mm at*
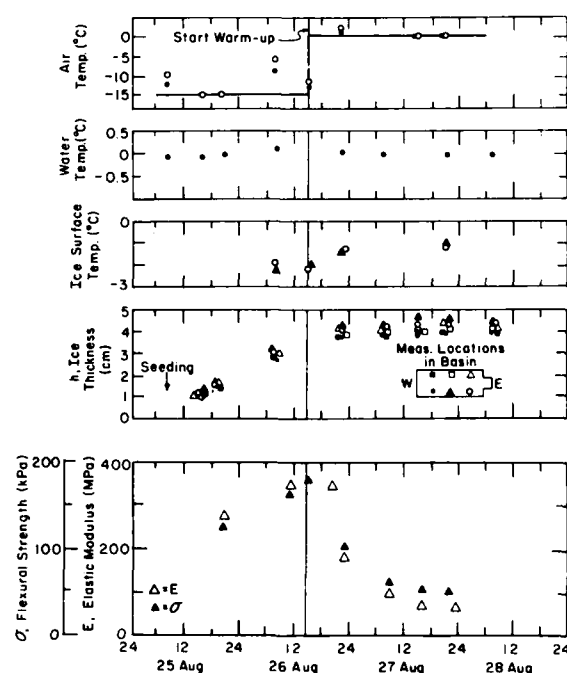
Figure 1. *Examples of measurements of ice characteristics (25–28 August 1981).*

2

the top of the sheet and increases in the direction of ice growth to about 5 mm at the bottom of a 7-cm-thick ice sheet. During ice growth, the air temperature in the room is kept at $-18°$ to $-10°C$ ($0°$ to $15°F$).

Ice sheets grown at the above air temperatures usually have too high a strength for tests at a model scale of 1/10 and lower. When the ice thickness is near the required value for a particular test, the ice is tempered by raising the air temperature in the room to approximately $2°C$ ($35°F$) for long enough to reduce the ice strength to the required value. This tempering or warm-up technique was first introduced by Schwarz (1975) for saline ice. During the study the ice thickness, ice strength, elastic modulus, surface temperature, and water temperature were monitored at regular intervals throughout the warm-up period. Examples of such measurements are shown in Figure 1.

Measurements

Temperature

As mentioned in the preceding section, water temperature was measured with a $1/50°C$ resolution thermistor. The air temperature in the room was continuously monitored and recorded by two thermocouples located immediately below the heat exchangers. During ice growth and tempering, the ice surface temperature was measured by thermistors mounted on a piece of Styrofoam.

Ice thickness

During ice growth the ice thickness was regularly measured with a caliper with 0.1 mm accuracy at six points along the perimeter of the test basin. After a test, the ice thickness near the track left by the tested structure was also measured to determine the distribution of ice thickness and to evaluate its degree of uniformity.

Ice flexural strength

The ice flexural strength σ was determined from in-situ cantilever beam tests. The beam width B was taken as one to two times the beam thickness H, and its length L was 6 to 7 times the thickness to minimize the buoyancy effects (Tatinclaux and Hirayama 1982) so that the formula for simple cantilever beams could be applied:

$$\sigma = \frac{6PL}{BH^2} \quad (1)$$

where P is the failure load applied at the free end of the beam. The load was usually applied by a 1-kg-capacity Chatillon push-pull gauge and occasionally by a motorized 50-lb-capacity load cell. For about ten ice sheets, beam tests were performed with the load applied both upward and downward for comparison purposes. For the other ice sheets, the load was applied only downward.

Elastic or strain modulus

In the present study, the elastic or strain modulus of ice E was measured by the plate deflection method recommended by Sodhi et al. (in press). Uniform loads were applied in incremental steps ΔP over a circular area of radius r near the center of the ice sheet, and the resulting incremental deflection $\Delta\delta$ of the ice sheet at the center of the load zone was measured by an LVDT. The characteristic length ℓ of the ice and its elastic modulus E were calculated according to the theory of an infinite plate on an elastic foundation:

$$\ell = \left\{ \frac{\Delta P}{8\,\gamma_w \Delta\delta} \left[1 + \frac{\alpha^2}{2\pi} \left(\ln \frac{\gamma\alpha}{2} - \frac{5}{4} \right) \right] \right\}^{1/2} \quad (2)$$

and

$$E = \frac{12\,(1-v^2)\,\gamma_w\,\ell^4}{H^3} \quad (3)$$

where γ_w is the specific weight of water, v is the Poisson's ratio of ice, taken equal to $1/3$, $\alpha = r/\ell$ and $\ln\gamma$ is the Euler's constant.

This method, which is nondestructive and simple to apply, proved to give consistent results. The set-up for load application and deformation measurement either in the upward or downward mode is shown schematically in Figure 2.

Urea concentration

Urea concentration in the tank water and in the ice was measured by a Beckman Blood-Urea-Nitrogen
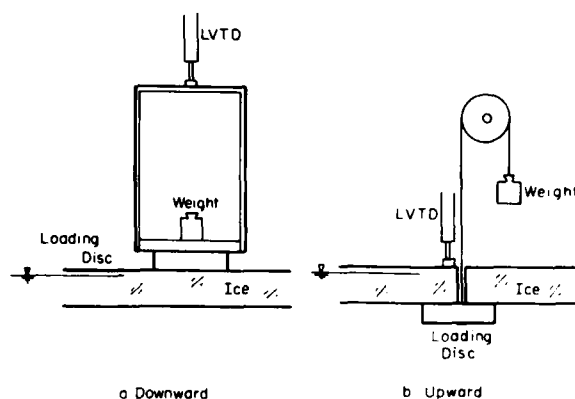
Figure 2. Experimental set-up for measurements of elastic modulus.

3

(BUN) Analyzer 2, which had been initially cali-
brated by urea solutions in distilled water of known
concentration.

ICE GROWTH AND STRUCTURE

Ice thickness distribution

Two examples of ice thickness distribution in the
test basin are shown in Figure 3. In these two ex-
amples, taken during the summer months, besides
local effects from the melting–recirculation tanks
at the north end of the tank and from the prep room
at the south end, the ice thickness can be observed
to increase slightly from the northwest corner to
the southeast corner of the basin. This trend was
reversed during the winter season; that is, the ice
increased in thickness from the southeast corner to
the northwest corner of the basin. The outsides of
the north and west walls are exposed to the atmos-
phere, while the south wall separates the basin from
the instrumentation corridor, where air conditioning
keeps the air temperature at 20°–25°C year-round.

Reasons for the slight nonuniformity in the ice thick-
ness which have been identified or are suspected are:

1. Uneven air temperatures outside the basin
   room (atmosphere, instrumentation cor-
   ridor, prep room).
2. Uneven temperature distribution and nat-
   ural convection in the basin room due to
   inadequate or uneven defrosting of the
   heat exchanger coils.
3. Excessive traffic in the room, resulting in
   excessive opening and closing of the doors.
4. Excessive heating of meltwater in the
   melting tank.
5. Inadequate operation of the pump recir-
   culation system.
6. Nonuniform air bubbling prior to seeding.

Reasons 2–6 can be greatly reduced if not totally
eliminated by careful operation of the ice test basin.
In addition, it was observed that the longitudinal
center portion (4 to 32 m) of the basin, where the
model tests are usually carried out, has a satisfactory
uniform ice thickness distribution. Table 1 presents
statistics of ice thickness distribution in the test

a. 6 July 1981.

b. 28 August 1981.
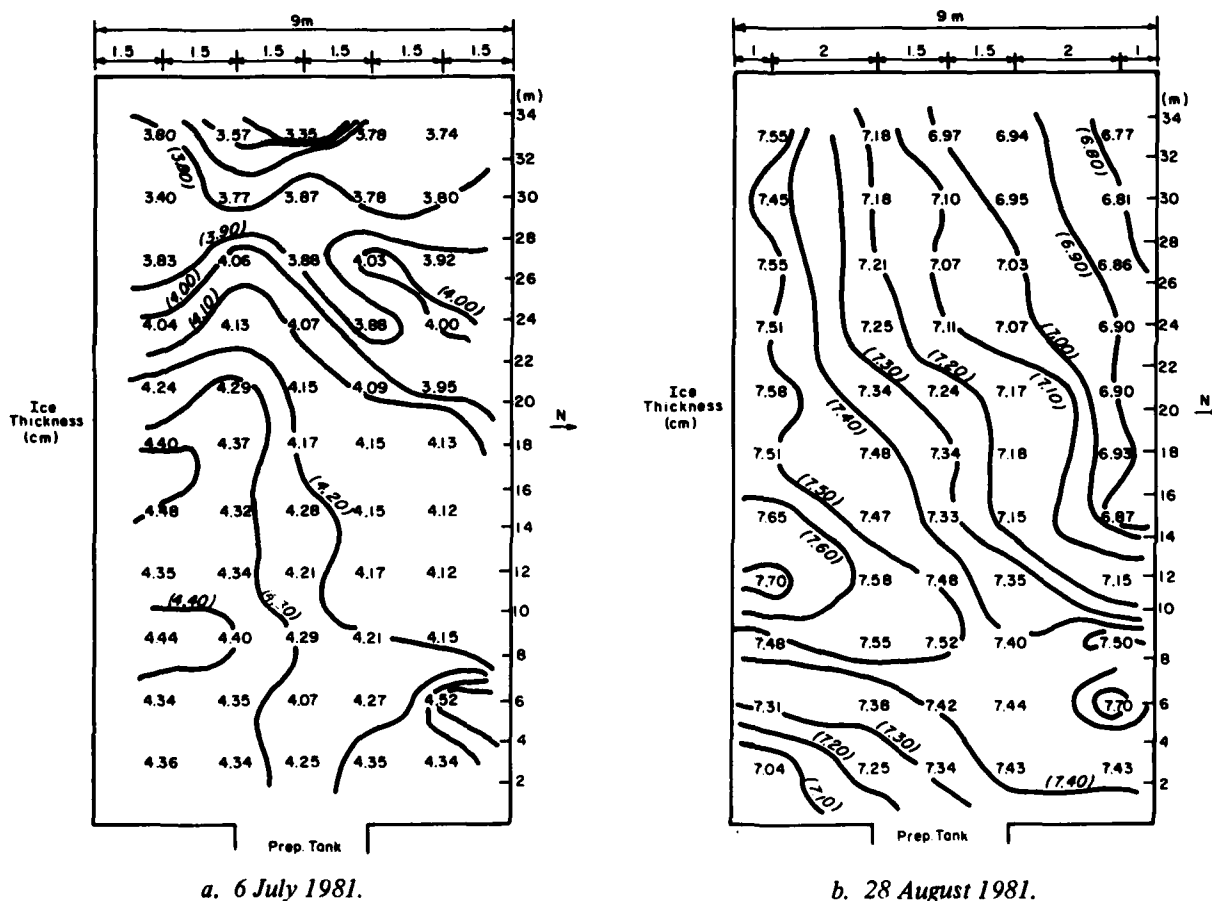
Figure 3. Examples of ice thickness distribution in tank.

4

Table 1. Statistical characteristics of ice thickness distribution.

Date	Measurement zone	No. of points	Mean (cm)	Std. dev. (cm)	Ice thickness max. (cm)	Ice thickness min. (cm)	Coef. of variation (%)
28 Aug	6–30 m	27	4.14	0.176	4.40	3.77	4.3
6 July	6–30 m	27	7.29	0.172	7.58	6.95	2.4
9 Sept	6–27 m	24	6.45	0.160	6.65	6.04	2.5
14 Sept	6–27 m	24	3.42	0.047	3.55	3.37	1.4
18 Sept	6–24 m	21	3.37	0.083	3.57	3.20	2.5
24 Sept	8–28 m	20	4.67	0.070	4.80	4.55	1.5
16 Nov	8–30 m	12	5.61	0.090	5.74	5.42	1.6
19 Nov	8–30 m	11	3.29	0.053	3.39	3.22	1.6
23 Nov	8–30 m	12	5.61	0.047	5.67	5.53	0.8
27 Nov	8–30 m	12	3.41	0.078	3.55	3.26	2.3
1 Dec	8–30 m	11	5.55	0.033	5.58	5.42	0.6
4 Dec	10–30 m	11	3.35	0.050	3.47	3.27	1.5

1.9%
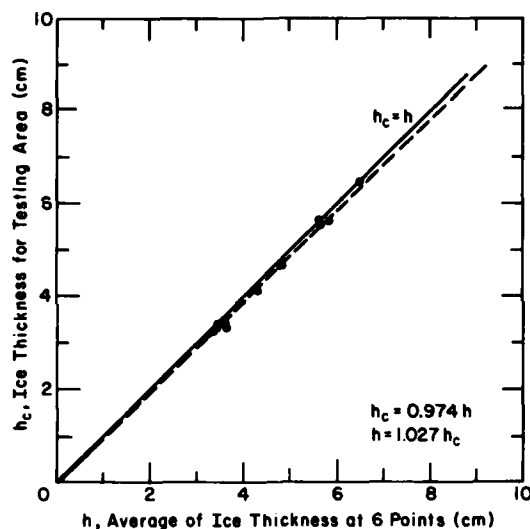
Figure 4. Average ice thickness in test area of tank versus average thickness at six points along the tank boundary.

portion of the basin. For most ice sheets the standard deviation in ice thickness is less than 1 mm, and of the order of 2% or less of the mean thickness. Finally, as shown in Figure 4, the mean ice thickness h_c in the test portion of the basin was practically equal to the average, h, of the thicknesses measured at the six points at the periphery of the basin shown in the insert of Figure 1. In the remainder of the report, this average thickness has been used as the nominal thickness of the ice sheet.

Ice growth during freeze-up

During ice growth the water at the tank surface and the air in the room are practically quiescent.

Therefore the classical relationship between ice thickness and negative degree-hours, found, for example, in Ashton's (1978) or Calkins's (1979) papers, for lake ice should be applicable, namely

$$h = \frac{1}{h_{ia}} \left\{ -k_i + \sqrt{k_i^2 - \frac{2h_{ia}^2 k_i}{\rho_i \lambda} \sum} \right\} \quad (4)$$

where

k_i = heat conductivity of ice
h_{ia} = heat transfer coefficient at ice/air interface
ρ_i = ice density
λ = latent heat of fusion of ice

$$\sum = \int_0^t (T_a - T_{iw}) \, dt$$

(T_a = air temperature, T_{iw} = freezing temperature of urea solution, t = time). Equation 4 assumes that there is no temperature gradient in the meltwater and that the temperature distribution in the ice sheet is linear, as shown in Figure 5. In Figure 6, the thicknesses of the ice sheets studied are plotted versus $(-\sum)$ in °C-hr, where

$$\sum = \int_0^t T_a \, dt \,.$$

That is, T_{iw}, the ice/water interface temperature or freezing temperature of the urea solution, was taken equal to 0°C, neglecting depression of the freezing point of the urea solution (0.155°C for a 0.5% solution and 0.31°C for a 1% solution) with respect to the freezing point of water. The data were separated into two sets. The first set (Fig. 6a) was obtained prior to August 1981 and the second (Fig. 6b) after

5

$$\phi_{ia} = h_{ia}(T_{ai} - T_a)$$

$$\phi_i = k_i \frac{T_{iw} - T_{ai}}{h}$$

T_a

AIR

T_{ai}

ICE

h

T_{iw} (freezing point of solution)

UREA SOLUTION
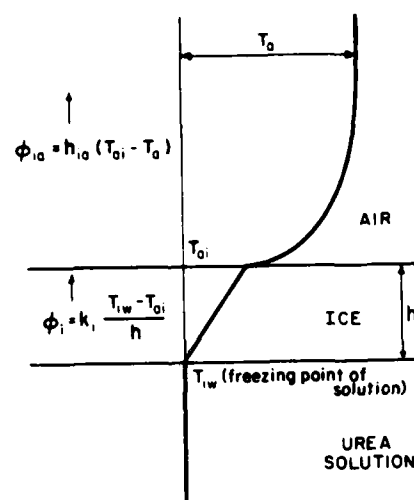
Figure 5. Definition sketch for heat transfer through a floating ice sheet.

o Apr 20-22	• Jun 26-29
△ Apr 23-24	+ Jun 30-Jul 1
◙ Apr 28-30	▣ Jul 2-6
▣ Apr 24-27	⊙ Jul 7-11
• May 4-6 (5°F)	◑ Jul 13-15
▲ May 6-8	⊙ Jul 22-25
▼ May 27-29	
▣ Jun 1-3	
▽ Jun 3-5	
⊙ Jun 5-8	
● Jun 8-11	
▣ Jun 11-15	
◑ Jun 17-19	
◐ Jun 19-22	
× Jun 24-26	

h, Ice Thickness (cm)

Eq 5

Eq. 4

with $\begin{cases} k_i = 19.3\,cal/°C\text{-}cm\text{-}hr \\ h_{ia} = 0.73\,cal/°C\text{-}cm^2\text{-}hr \\ \rho_i = 0.92\,g/cm^3 \\ \lambda = 79.8\,cal/g \end{cases}$

$-\Sigma$ (°C·hr)

a. Prior to August 1981.

o Aug 18-21
• Aug 22-28
△ Aug 29-Sep1
▲ Sep 3-9
✕ Sep 10-14
□ Sep 14-18
◙ Sep 19-21
+ Sep 26-28
◙ Oct 6-12
▽ Oct 16-21
⊙ Nov 12-16 (No 1)
◙ Nov 17-19 (No 2)
✦ Nov 19-23 (No 3)
● Nov 25-27 (No 4)
▼ Nov 27-Dec 1 (No 5)
▼ Dec 1-3 (No. 6)

h, Ice Thickness (cm)

Eq 5

Eq 4

with $\begin{cases} k_i = 14.85\,cal/°C\text{-}cm\text{-}hr \\ h_{ia} = 0.81\,cal/°C\text{-}cm^2\text{-}hr \\ \rho_i = 0.92\,g/cm^3 \\ \lambda = 79.8\,cal/g \end{cases}$

$-\Sigma$ (°C·hr)

b. After August 1981.

Figure 6. Relationship between ice thickness and degree-hours.

6

August 1981, when control of water temperature at seeding and frequency of heat exchanger defrosting were improved. As can be seen from the two figures, these improvements resulted in a slightly larger growth rate of the ice and in a significant reduction in the scatter of the data points. Lines corresponding to equation 4 were fitted through the data points in Figure 6. In Figure 6a, the heat conductivity of ice was assumed to be that of freshwater ice, i.e. $k_i = 19.26$ cal/°C-cm-hr, and h_{ia} was calculated by nonlinear regression analysis of the experimental data and found equal to

$$h_{ia} = 0.73 \text{ cal/hr-cm}^2\text{-}°C .$$

In Figure 6b, both k_i and h_{ia} were calculated by nonlinear regression analysis to be

$$k_i = 14.85 \text{ cal/°C-cm-hr}$$

$$h_{ia} = 0.81 \text{ cal/°C-cm}^2\text{-hr} .$$

In these calculations it was assumed that $\lambda = 79.8$ cal/g and $\rho_i = 0.92$ g/cm³.

As also shown in Figure 6, for ice thickness less than 2 to 3 cm, eq 4 can be approximated by a linear relationship

$$h = -\frac{h_{ia}}{\rho_i \lambda} \sum \tag{5}$$

as proposed by Assur and Weeks (1964).

Ice growth during warm-up

It was observed that during the warm-up or tempering period necessary to achieve the ice strength required for a particular model scale, the ice thickness continued to increase slightly. Let h_i be the ice thickness at the start of the warm-up period when room refrigeration is discontinued and the air temperature is allowed to rise above freezing, and $h(t)$ the ice thickness at any subsequent time. The relative increase in thickness

$$\frac{\Delta h}{h_i} = \frac{h(t) - h_i}{h_i}$$

has been plotted versus t/h_i^2 in Figure 7. The parameter t/h_i^2 was selected on the basis of the study by Schwarz and Miloh (1972), who showed that the time necessary for a saline ice sheet initially at uniform temperature to reach equilibrium temperature when one face of the ice is suddenly brought to a different temperature T_A is independent of T_A and of the ice salinity but inversely proportional to the square of the ice thickness. In spite of the scatter in the data points, Figure 7 shows that $\Delta h/h_i$ increases asymptotically toward a value of approximately 0.20. The equation of the curve in Figure 7 was obtained by nonlinear regression analysis as

$$\frac{\Delta h}{h_i} = \frac{0.22 \, t/h_i^2}{t/h_i^2 + 0.57} . \tag{6}$$

The final ice thickness h_f at which the model tests were conducted is plotted versus the initial ice thickness h_i in Figure 8. It can be seen that the data points lie on a straight line:

$$h_f = 1.17 \, h_i . \tag{7}$$

Figure 7. Relative increase of ice thickness during warm-up.
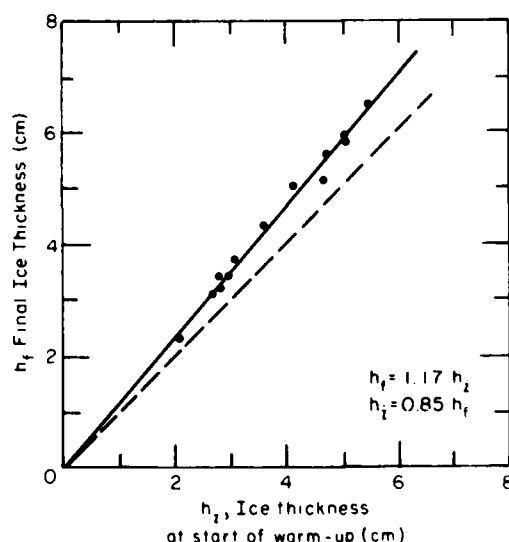
Figure 8. Final ice thickness versus initial ice thickness at start of warm-up.

7

Top Layer
(1.3 cm)

Bottom
Layer
(4.6 cm)

Scale (mm)

(a)

(b)

(c)

(d)

(e)

Scale

1 mm
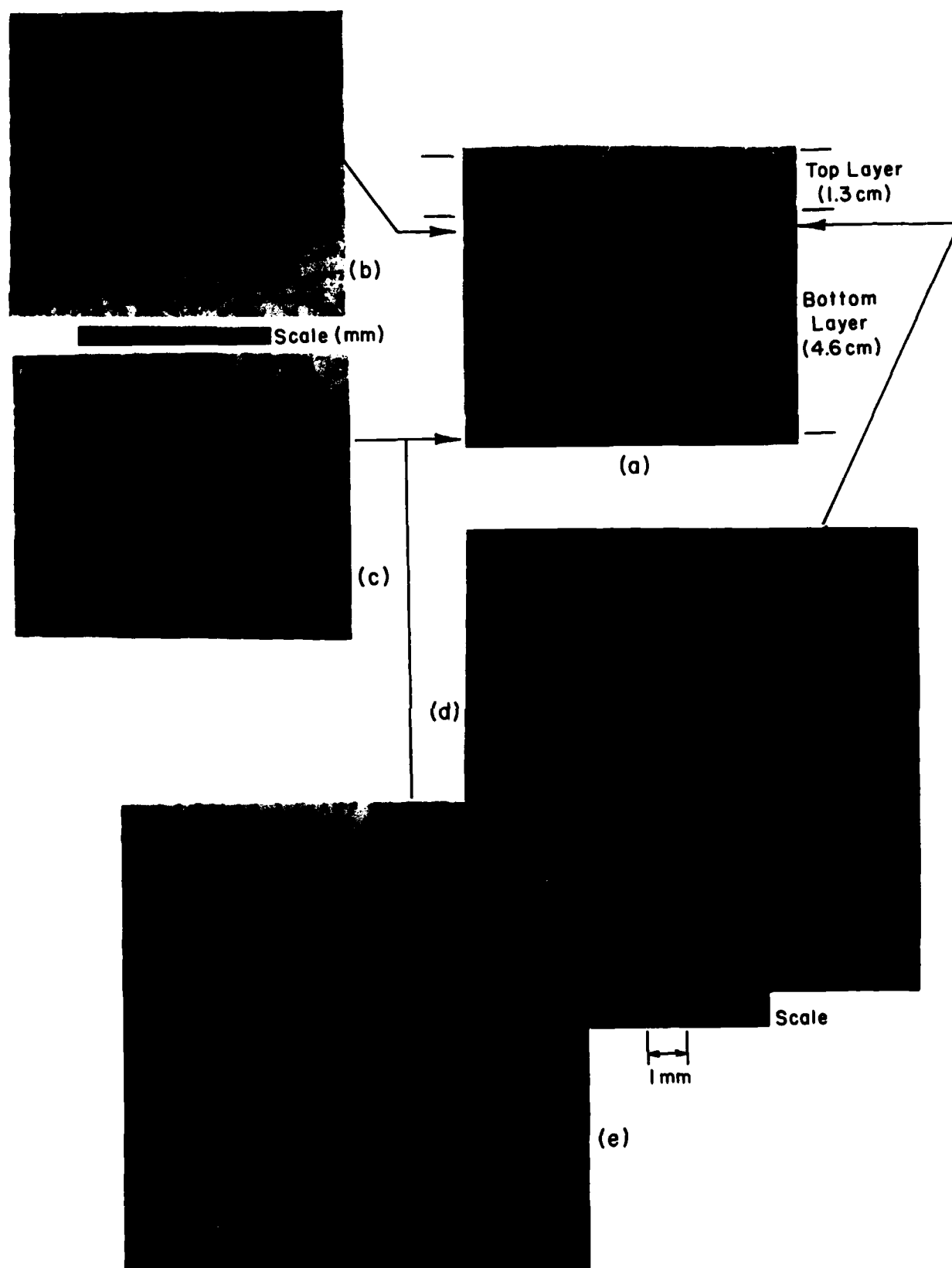
Figure 9. Thin sections of urea-doped ice (courtesy of A. Gow).

Because there is less scatter in Figure 8 than in Figure 7, eq 7 may be more reliable than eq 6 for predicting the ice thickness at which warm-up should be started to achieve a desired final ice thickness as long as the test conditions are within the limits of those investigated in the present study.

Structure of urea-doped ice

Photographs of thin sections of urea-doped ice are shown in Figure 9. It can be seen that urea-doped ice is similar to natural sea ice insofar as it contains distributed brine-like cells (see Fig. 9b). However, contrary to sea ice, the urea-doped ice grown in the CRREL basin is composed of two distinct layers, as evidenced in Figure 9a. The thicker bottom layer has a c-axis-horizontal, columnar structure characteristic of dendritic growth, while the thinner top layer is made of much shorter columns with mixed vertical and horizontal c-axis orientation. As is obvious in Figure 9a, there is a distinct discontinuity in crystal structure at the interface between the top and bottom layers. The thickness of the top layer of urea-doped ice is relatively much larger than that of the transition incubation layer in normal sea ice.

The growth of urea-doped ice may be compared to the congelation process of metal alloy melts as studied by Tiller (1958). If the analogy is valid,

a. c = 1.05%.

b. All urea concentrations.
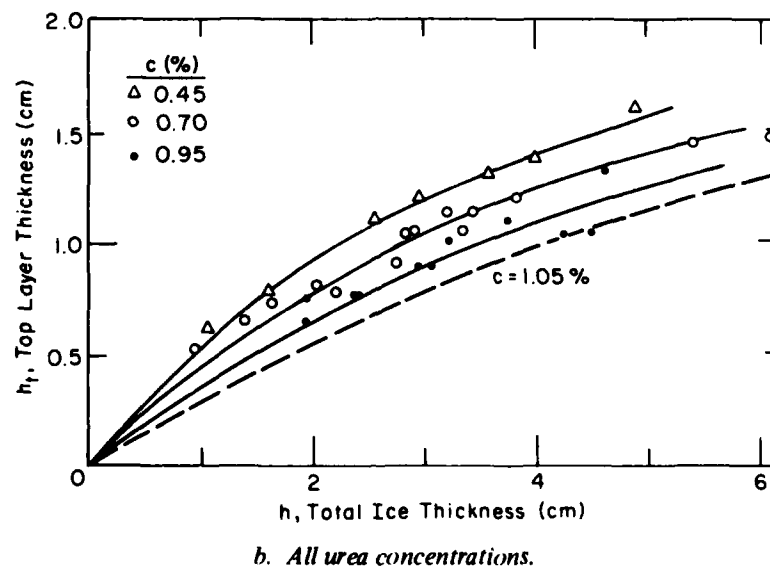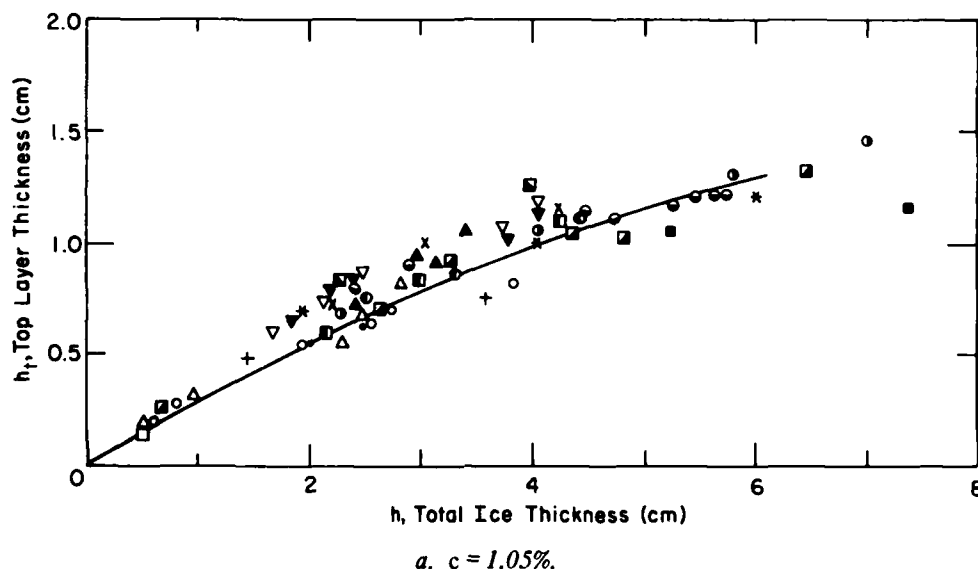
Figure 10. Top layer thickness vs total ice thickness.

9

according to Tiller columnar growth of urea ice takes place when the following instability condition is satisfied:

$$\frac{G}{R} < \frac{m\,c_0\,(1-k)}{D\,k} \qquad (8)$$

where

G = temperature gradient in the liquid at the freezing interface

R = growth rate

k = equilibrium partition coefficient of the solute

m = liquidus slope (a negative quantity)

D = diffusion coefficient

c_0 = initial concentration of solution.

The thickness h_t of the top layer with random c-axis orientation of the crystals is given by Tiller (1958) as

$$h_t = -\frac{D}{kR}\ln\left[1 - \frac{G\,D\,k}{c_0\,R\,m\,(1-k)}\right]. \qquad (9)$$

It is uncertain whether this equation is applicable to the case of very thin urea-doped ice where connections between brine cells are possible and brine migration is to be expected. Moreover, it has been observed, as discussed in the following section, that the thickness of the top layer of model ice continues to increase during the growth of the ice sheet. This puzzling phenomenon remains unexplained, but would imply a recrystallization process at the interface between the top and bottom layers of the model ice. The increase in top layer thickness with increasing total ice thickness is illustrated in Figure 10a for the 1.05% urea concentration and in Figure 10b for the other three concentrations investigated. In these figures it is evident also that the ratio h_t/h decreases with increasing urea concentration, and decreases
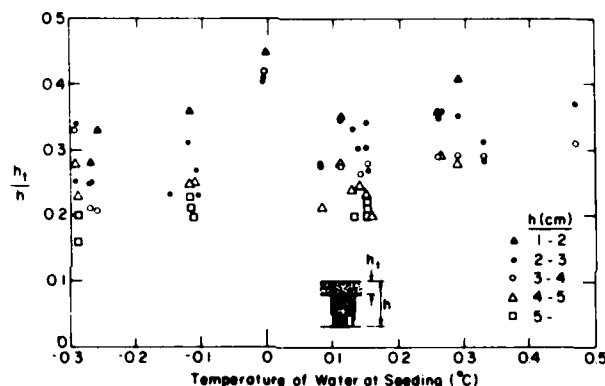
Figure 11. Effect of water temperature at time of seeding on top layer thickness (c = 1.05%).

Table 2. Urea concentration in ice and water solution.

Date	Time	Ice thickness h (cm)	Top	Bottom	Solution	Remarks
1 Sept		5.8	0.07	0.16	0.44	
11 Sept	1200	3.2	0.17	0.32	0.68	
12 Sept	1030	3.6	0.15	0.28		
13 Sept	1800	3.6	0.13	0.25		Warm-up period
27 Sept		3.0	0.30	0.51	0.91	
20 Nov	0830	2.0	0.20	0.41	0.91	
21 Nov	0730	5.0	0.25	0.42		
8 Oct	1030	4.3	0.25	0.50		
8 Oct	1800	4.7	0.27	0.42		
27 Nov	0900	2.1	0.29	0.44	0.91	
28 Nov	1830	2.9	0.28	0.44		
29 Nov	1200	4.8	0.25	0.44		
30 Nov	0900	5.5	0.19	0.36		Warm-up period
1 Dec	0700	5.6	0.22			

with increasing thickness h toward an asymptotic value varying between 0.2 and 0.3. One other parameter which was found to affect the top layer thickness is the water temperature at seeding. Figure 11, for the particular urea concentration of 1.05%, shows an increase in the ratio h_t/h with increasing water temperature at seeding. The observed variations of h_t with urea concentration and water temperature at seeding are in qualitative agreement with eq 9.

Finally, because of the difference in their crystal structure, the urea concentrations in the top and bottom layers are expected to be different. This was confirmed by measurements listed in Table 2, where it can be seen that during the freeze-up period the urea concentration in the top layer is of the order of half that in the bottom layer, itself about half the urea concentration in the basin water. Once warm-up of the ice sheet was started, the urea concentration in both layers was observed to decrease, which indicates an increase in cavities within the ice, leading to drainage and loss of urea.

MECHANICAL PROPERTIES OF UREA-DOPED ICE

Introductory remarks

Studies on the mechanical properties of saline ice, namely bending strength and strain modulus, have shown that these properties are functions of many parameters, such as rate of loading, solute concentration in the meltwater, ice temperature, direction of load application, and even method of measurement. In the present study, all the measurements were made in situ. As mentioned earlier, the bending strength was measured in small cantilever beam tests, and the strain modulus by the plate deflection method. In the majority of the cantilever beam tests, the load was applied manually and at such a rate that

Figure 12. Relationship between ice surface temperature and air temperature.

beam failure occurred within 1 to 2 seconds, following the recommendations of the IAHR Committee on Ice Problems. Since the tests were performed in situ, the bottom of the ice was always at melting temperature, and only the ice surface temperature could be varied, by varying the ambient air temperature. Figure 12 shows that a variation of some 12°C (22°F) in air temperature results in a variation of only about 2°C (3.6°F) in the ice surface temperature.

In addition to the effects of air temperature, urea concentration and direction of loading on ice properties, the influence of the two-layer structure of the ice on the model ice properties can be, at least qualitatively, predicted by a mathematical model, presented below.

Last but not least is the effect of tempering or warm-up on the mechanical properties of urea-doped ice. The effect of warm-up was investigated at great length in order to be able to predict the warm-up duration necessary to achieve the required mechanical properties, primarily bending strength, and consequently to establish in advance a reliable schedule for ice freeze-up, ice tempering, and ultimately the test program.

The experimental data on the mechanical properties of untempered urea-doped ice have been tabulated in Appendix B and those for tempered ice in Appendix C.

Model of a two-layer elastic material

Consider a sheet of thickness H of a nonhomogeneous material composed of two layers. The top layer, of thickness aH, is a homogeneous, elastic material characterized by its bending strength σ_1 and elastic modulus E_1. The bottom layer, of thickness $(1-a)H$, is characterized by σ_2 and E_2, with $\sigma_1 > \sigma_2$ and $E_1 > E_2$ (see Fig. 13).

A cantilever beam of length L and width B of this composite material is subjected to a load P at the free end. It is assumed that the strain distribution $\epsilon(z)$ across the beam is linear, as shown in Figure 13, i.e.

$$\epsilon(z) = \epsilon_t z/z_0 \qquad (10)$$

where ϵ_t is the strain at the top surface of the beam, z is measured positive upward from the yet-undetermined neutral axis, and z_0 is the distance from the neutral axis to the beam top surface.

The stress distribution in the top layer is given by

$$\sigma^{(1)} = E_1 \epsilon = E_1 \epsilon_t \frac{z}{z_0}$$

or

$$\sigma^{(1)} = \sigma_t \frac{z}{z_0} \qquad (z_0 - aH < z < z_0) \qquad (11)$$
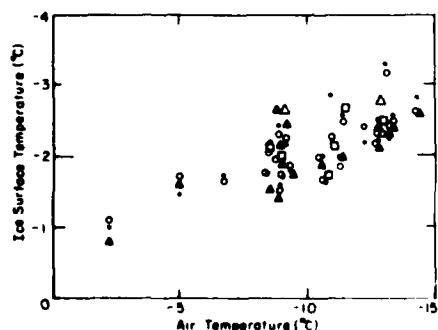
11
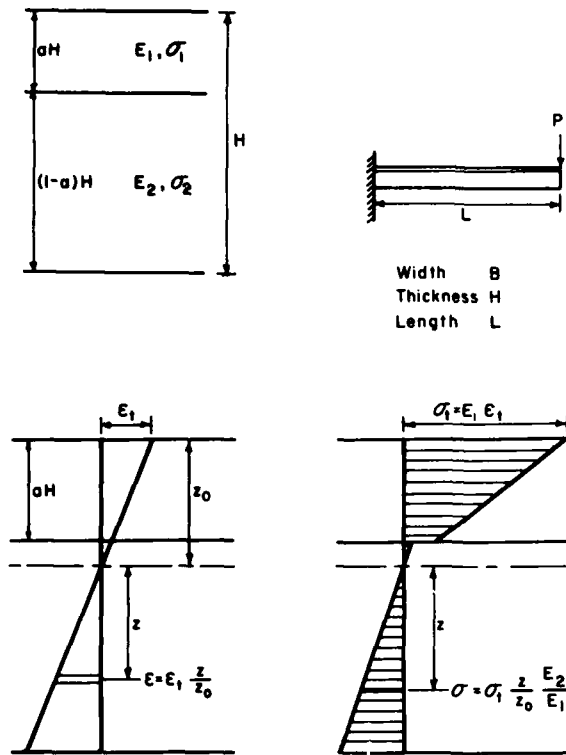
Figure 13. Definition sketches for two-layer model.

where σ_t is the stress at the top surface. In the bottom layer the stress distribution is given by

$$\sigma^{(2)} = E_2 \epsilon = \frac{E_2}{E_1} \sigma_t \frac{z}{z_0} \qquad (z_0 - aH < z < H).$$

(12)

From the condition $\int \sigma dz = 0$, the position of the neutral axis is found to be

$$z_0 = \frac{H}{2} \frac{1 - a^2 + a^2 b}{1 - a + ab}$$

(13)

where $b = E_1/E_2$.

If E_0 is the elastic modulus of the equivalent homogeneous beam, i.e. which experiences the same tip displacement δ under the same load P, then

$$E_0 I = E_1 I_1 + E_2 I_2$$

(14)

where $I = BH^3/12$ is the beam moment of inertia about its mid-thickness and I_1 and I_2 are the moments of inertia of the top layer and bottom layer, respectively, about the actual neutral axis. Equation 14 yields

$$\frac{E_0}{E_1} = a^3 + \frac{(1-a)^3}{b} + \frac{3a(1-a)}{1-a+ab}.$$

(15)

Application of eq 15 to measurements carried out on urea-doped ice beams and their top layers alone (i.e. after scraping off the bottom layer) yielded values of E_1/E_2 of 20 or more.

When the load P is applied downward, failure occurs when the stress at the top of the beam σ_t becomes equal to the tensile strength σ_1 of the top layer material. Let σ_0 be the nominal strength of the equivalent homogeneous beam with neutral axis at mid-thickness, i.e. calculated from eq 1 with $h = H$; it can be shown that

$$\frac{\sigma_0}{\sigma_1} = \frac{H}{2z_0} \frac{E_0}{E_1}.$$

(16)

When the load P is applied upward, it can be expected that a crack forming at the bottom of the beam when the stress there becomes equal to σ_2 will propagate up to the interface between the top and bottom layers. Total failure of the beam will then occur when the stress at the interface becomes equal to σ_1. The corresponding nominal strength σ_0' of the composite beam calculated from eq 1 with $h = H$ is such that

$$\frac{\sigma_0'}{\sigma_1} = a^2.$$

(17)

Therefore, when such a two-layer beam is tested in both the downward and upward modes, the ratio of the corresponding strengths given by application of simple beam theory (eq 1) is given by

$$\frac{\sigma_0'}{\sigma_0} = 2a^2 \frac{z_0}{H} \frac{E_1}{E_0}.$$

(18)

The reasoning which led to eq 17 and 18 should be valid for urea-doped ice, where the bottom layer, with its columnar structure and the brine pockets it contains, offers little resistance to tension, especially during warm-up.

The nominal ratio E_0/σ_0 can be obtained in terms of the ratio E_1/σ_1 for the top layer from eq 13 and 16 as

$$\frac{E_0/\sigma_0}{E_1/\sigma_1} = 2\frac{z_0}{H} = \frac{1 - a^2 + a^2 b}{1 - a + ab}.$$

(19)

Equations 13, 15, 16 and 18 have been plotted in Figure 14 with a as the variable and for the particular value $E_1/E_2 = 20$. It can be noted that, according to the above model, over a fairly wide range of the parameter a (approximately $0.1 < a < 0.4$) both the ratios σ_0/σ_1 and E_0/E_1 remain nearly constant, while the ratio σ_0'/σ_0 varies significantly from 0.03, at $a = 0.1$, to 0.47, at $a = 0.4$, for the particular value of

12
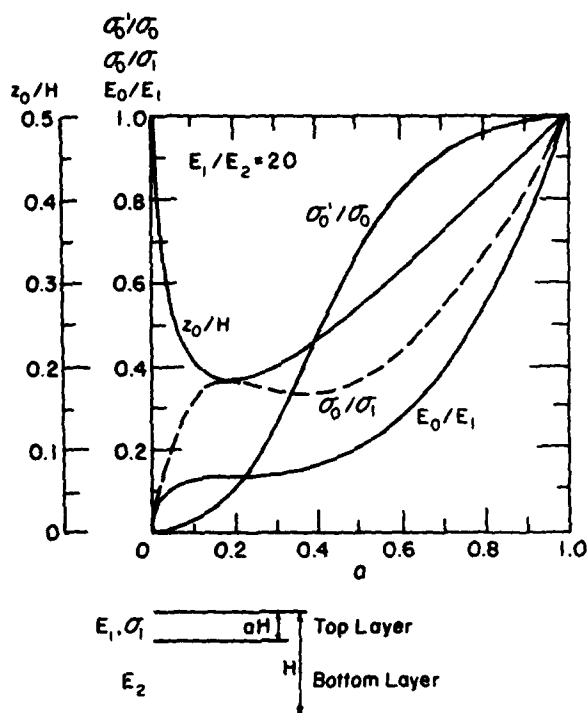
Figure 14. *Variation of properties of a two-layer material with relative thickness of top layer.*

Figure 15. *Variation of flexural strength with ice thickness and air temperature during freeze-up (c = 1.05%).*

$E_1/E_2 = 20$. This range of a does include the values of h_t/h of 0.2 to 0.3 observed for the urea-doped ice investigated in the present study.

Finally, it can be inferred from Figure 14 that, according to the double layer model, when a low value of σ_0, i.e. of σ_0/σ_1, is required together with a high value of E_0/σ_0, i.e. of $(E_0/\sigma_0)/(E_1/\sigma_1)$, the top layer should be very thin, of the order of 5% or less of the total thickness.

Properties of urea-doped ice during freeze-up

The measurements of ice thickness, and ice mechanical properties performed during freeze-up, have been regrouped in Table 3 for easier reference.

Flexural strength

Figure 15 presents results for measurements of the flexural strength σ (in the downward mode) for ice grown from a 1.05% urea solution. The results pertain to several ice sheets grown at various air temperatures, and measurements were taken at different ice thicknesses during the freezing period. In spite of the unavoidable scatter in the data, it is apparent that the flexural strength increases with decreasing air temperature, i.e. with decreasing ice surface temperature. As mentioned previously, a drop of about $11°C$ ($20°F$) in air temperature T_a resulted in a drop

of about $2°C$ ($4°F$) in ice surface temperature. This in turn translated into an increase in ice strength of the order of 30 kPa, from 50–60 kPa at $T_a > 7°C$ ($20°F$) to 80–100 kPa at $T_a < -12°C$ ($10°F$) for an ice thickness of about 3 cm, as can be seen from Figure 15.

Figure 15 also shows an increase in flexural strength with ice thickness, which parallels the increase in top layer thickness with total thickness (Fig. 10), thereby further indicating the important effect of the top layer on the nominal flexural strength of the ice.

A similar increase of flexural strength with ice thickness was observed with the ice sheets grown from solutions of varying urea concentration as evidenced in Figure 16, where the ice sheets were grown at an air temperature between -12° and -9°C (10° and 15°F. Average empirical relationships between ice strength and ice thickness were calculated by a
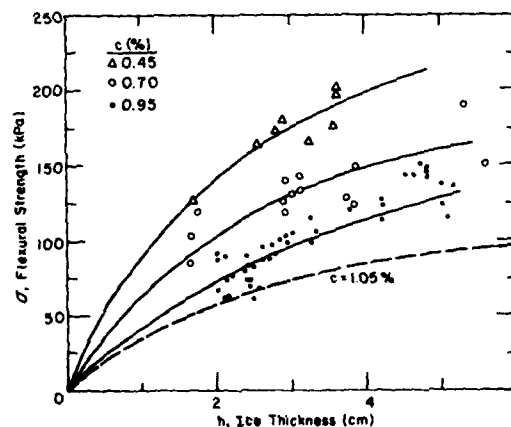
Figure 16. *Variation of flexural strength with ice thickness during freeze-up (all urea concentrations).*

13

Table 3. Summary of measurements during freeze-up.

C%	Date	Time	$\bar{\sigma}$ (kPa)	σ'(kPa)	E(MPa)	E'(MPa)	h(cm)	h_t(cm)	σ'/σ	$E/\sigma \times 10^{-3}$	h_t/h
1.05	28 May	0900	44.0				2.34	0.72			0.31
		1400	34.7				2.93	0.88			0.30
	28 May	2100	32.1				3.16	0.91			0.29
	29 May	0800	23.0				3.40	1.05			0.31
		1400	20.3		31.6					1.56	0.31
	2 June	0900	67.6				1.69	0.61			0.36
		1600	83.9				2.43	0.84			0.35
	3 June	0900	84.0				3.72	1.08			0.29
		1200	85.1				4.01	1.18			0.29
	4 June	1030	66.6		91.7		1.85	0.68		1.37	0.36
		1630	78.2				2.38	0.83			0.35
	5 June	0830	87.1				3.75	1.03			0.27
		1100	100.6				4.03	1.13			0.28
	6 June	0800	49.7				1.73	0.71			0.41
		2030	63.6				2.82	0.98			0.35
	7 June	0900	66.7				3.76	1.10			0.29
		1900	67.0				4.44	1.25			0.28
	8 June	0830	94.0				5.34	1.45			0.27
		1100	75.0				5.61	1.53			0.27
1.05	10 June	0900	74.3				2.52	0.75			0.30
		1630	74.4		62.8		3.31	0.87		0.84	0.26
	11 June	0830	90.8		59.8		4.43	1.10		0.66	0.23
	13 June	2300	48.9		43.7		3.89	0.88		0.89	0.23
	14 June	0930	88.1				5.24	1.06			0.20
	15 June	0930	79.9				7.38	1.16			0.16
		1200	163.9		16.3					1.13	0.16
	18 June	0900	53.7				2.66	0.72			0.27
		1600	60.8				3.26	0.91			0.28
	19 June	0900	93.6				4.82	1.03			0.21
	20 June	0800	68.2				2.14	0.72			0.34
	21 June	0800	89.8				4.34	1.05			0.24
	22 June	0900	90.8				6.67	1.31			0.20
	25 June	0830	62.9				2.21	0.76			0.34
	26 June	0800	91.9				4.25	1.16			0.27
	27 June	0800	52.3				1.92	0.69			0.36
	28 June	0800	81.0				4.00	1.00			0.25
	29 June	0800	89.7				6.01	1.21			0.20
		1130	76.6								
1.05	1 July	0800	86.8				3.57	0.76			0.21
	3 July	1130	58.0					2.77			0.31
	4 July	1030	74.8				4.02	1.05			0.26
	5 July	1330	92.7				5.80	1.31			0.23
	6 July	0900	123.2				6.98	1.45			0.21
		1230	94.9		84.6					0.89	0.21
		1400	80.2		74.0					0.92	0.21
	8 July	1300	90.7		59.7		2.91	0.89		0.66	0.31
	9 July	0800	87.0		93.9		4.73	1.10		1.08	0.23
	15 July	0800	94.0				2.80	1.14			0.41
		0930	98.6				3.00	1.28			0.43
	20 July	0900	84.2				3.66	1.41			0.39
	21 July	0800	88.2		134.0		4.71	1.64		1.52	0.35
	24 July	0830	77.9		51.0		4.00	1.23		0.63	0.31
0.45	19 Aug	0900	76.2		40.8		2.08	1.07		5.35	0.51
	25 Aug	2030	126.5	85.2	27.1		1.60	0.79	0.67	2.14	0.49
	26 Aug	1100	167.1	104.9	33.7		2.93	1.22	0.63	2.01	0.42
		1500	203.6	81.3	34.1				0.40	1.67	
	30 Aug	0930	173.4	76.4	220.5		2.?6	1.11	0.44	1.27	0.43
		1900	193.4	90.9	311.9		3..?	1.31	0.47	1.61	0.37
	31 Aug	0900	167.1	99.8	306.5		4.?	1.60	0.60	1.83	0.33

C%	Date	Time	$\bar{\sigma}$ (kPa)	σ' (kPa)	E(MPa)	E'(MPa)	h(cm)	h_t(cm)	σ'/σ	E/σ $\times 10^{-3}$	h_t/h
0.70	6 Sept	1000	137.7	74.6	187.3	176.5	2.91	1.05	0.54	1.36	0.36
		1800	133.8	90.3	169.3	191.8	3.82	1.20	0.68	1.27	0.31
	7 Sept	0830	171.7	80.3	178.8	181.7	5.42	1.45	0.47	1.04	0.27
	10 Sept	2130	102.2	58.1		185.8	1.61	0.74	0.57	1.82	0.46
	11 Sept	0900	125.0	64.5	180.3	189.6	2.85	1.04	0.52	1.44	0.36
	15 Sept	0930	87.1	50.4	69.1		2.02	0.81	0.58	0.79	0.40
	20 Sept	0800	65.1	49.2	68.7	70.9	2.76	0.91	0.76	1.06	0.33
0.95	27 Sept	0900	66.5	35.1	79.0	86.0	2.38	0.76	0.53	1.19	0.32
	7 Oct	1300	76.4	35.0	78.4		2.36	0.76	0.46	1.03	0.32
	8 Oct	0900	122.5	47.6	80.8		4.25	1.06	0.39	0.66	0.24
	17 Oct	2130	81.6	43.7	118.4		1.93	0.75	0.54	1.45	0.39
	18 Oct	1600	106.9	53.5	131.1		3.21	1.00	0.50	1.23	0.31
		2000	121.5	56.1	122.5		3.75	1.09	0.46	1.01	0.29
	19 Oct	0900	163.5	59.4	158.2		4.61	1.32	0.41	1.10	0.29
	13 Nov	0800	81.2				1.99	0.58			0.29
	14 Nov	1030	124.8				5.15	1.00			0.19
	18 Nov	0800	94.3		62.2		2.71	0.69		0.66	0.26
	20 Nov	1200	87.2		66.0		1.99	0.61		0.76	0.31
	21 Nov	0830	143.7		187.9		4.92	1.07		1.31	0.22
	26 Nov	0800	92.1		74.8		2.56	0.68		0.81	0.27
	28 Nov	0900	60.8		45.8		1.99	0.73		0.75	0.37
		1800	103.0		88.7		2.87	0.85		0.86	0.30
	29 Nov	1800	146.2		182.7		4.80	1.08		1.25	0.23
	2 Dec	1200	91.0		64.2		2.76	0.73		0.71	0.26

nonlinear regression analysis of the data presented in Figure 15 ($-12°C < T_a < -9°C$) and Figure 16 as

$$c = 1.05\% \qquad \sigma = \frac{142\,h}{h + 2.84} \qquad (20a)$$

$$c = 0.95\% \qquad \sigma = \frac{261\,h}{h + 5.06} \qquad (20b)$$

$$c = 0.70\% \qquad \sigma = \frac{256\,h}{h + 2.88} \qquad (20c)$$

$$c = 0.45\% \qquad \sigma = \frac{329\,h}{h + 2.61} \qquad (20d)$$

where h is expressed in cm and σ in kPa. Curves corresponding to the above equations are drawn in Figures 15 and 16.

Figure 16 shows a significant increase in flexural strength with decreasing urea concentration in the melt solution. For example, for 2-cm-thick ice the measured flexural strengths at urea concentrations of 0.45%, 0.7%, 0.95% and 1.05% were 130 kPa, 100 kPa, 70 kPa and 50 kPa, respectively, and for 6-cm-thick ice, the corresponding flexural strengths were about 210 kPa, 150 kPa, 130 kPa and 90 kPa, respectively. To further illustrate the effect of urea concentration c on bending strength, values of σ predicted by eq 20 are plotted versus c for four ice thicknesses in Figure 17. It can be seen that σ is a decreasing linear function of c. A nonlinear regression analysis of the data in Figures 15 and 16, which

assumed a linear relationship between σ and c, yielded the following empirical relationship:

$$\sigma = \frac{291\,(1.55 - c)\,h}{h + 2.95} \qquad (21)$$

where c is expressed in percent, h in cm and σ in kPa.
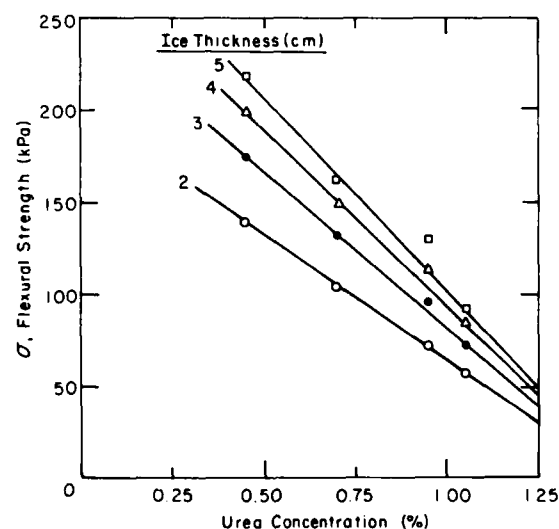
Figure 17. Variation of flexural strength during freeze-up with urea concentration in water and ice thickness.

15
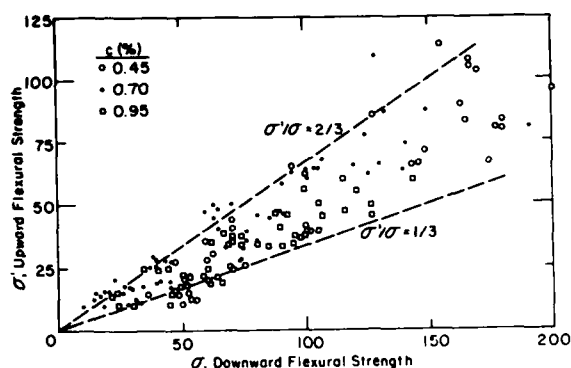
Figure 18. *Effect of loading direction on measured flexural strength.*
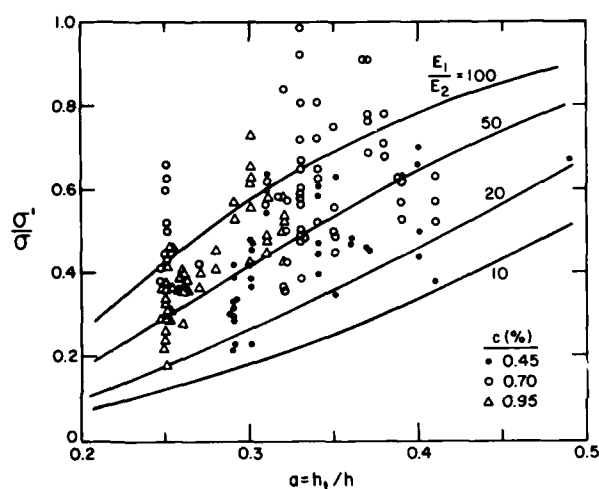
Figure 19. *Variation of σ'/σ with relative top layer thickness h_t/h.*

The effect of the direction of load application on the flexural strength calculated from cantilever beam tests according to eq 1 is evidenced in Figure 18, where σ', the strength obtained with upward loading, i.e. with the ice bottom in tension, is plotted against σ, the strength calculated under downward loading, i.e. with the top surface of the ice in tension. In Figures 18 and 19 the data presented were obtained during both freeze-up and warm-up. The corresponding values of σ'/σ were found to vary from as low as 0.20 to as high as 1.0 (in one instance only), with 80% of the data falling between 1/3 and 2/3. The values of σ'/σ have been plotted versus h_t/h, the ratio of top layer thickness of total ice thickness, in Figure 19, where lines corresponding to eq 18 of the proposed two-layer model have been drawn for various values of E_1/E_2. It can only be said that the experimental data exhibit a general increase of σ'/σ with h_t/h as predicted by the model. It is worth

mentioning that measurements performed on freshwater ice also showed that the strength σ' obtained by upward loading is also about 80% of the strength σ obtained by downward loading (see e.g. Timco and Frederking 1981). This difference is usually attributed to a difference in ice crystal size between the top and bottom surfaces of the ice. This is characteristic also of urea-doped ice, but was not taken into consideration in the proposed two-layer model, which assumes uniform, isotropic properties in each of the two layers.

During the period July–October of 1981, systematic ice strength measurements were performed at three locations along the south wall of the tank and at various times during freeze-up and warm-up. At each of the three locations, four cantilever beam tests were carried out to verify the repeatability of the results; comparison of the results obtained at the three locations at any given time would permit a check of the uniformity of ice strength in the tank. In all, 137 sets of four beam tests were carried out at 47 different times. The results of these tests have been listed in Appendixes B and C. For each set of four tests at one location and at one time, the local mean ice strength, local standard deviation and local coefficient of variation, i.e. the ratio of standard deviation to mean strength, were calculated. Similarly, for each of the 47 test times, the overall mean strength, overall standard deviation and overall coefficient of variation were also calculated. The results of these computations are listed in Table 4, and the histograms of the local and overall coefficients of variation are shown in Figures 20 and 21, respectively. The mean local coefficient of variation was 7.94% with a standard deviation of 5.65%, and the overall coefficient of variation was 6.31% with a standard deviation of 4.54%. These results indicate satisfactory repeatability and uniformity in the ice strength measurements, especially when compared with similar results available in the literature on ice testing.

Elastic modulus

The elastic modulus of an ice sheet in the test basin was measured by the plate deflection method. In most cases the load was applied near the center of the basin. In one instance, the uniformity of the elastic modulus was checked by repeating the measurements at 18 different locations in the tank. The results of this check are given in Figure 22; the mean elastic modulus was found to be 54.8 MPa, with a standard deviation of 5.2 MPa or about 10% of the mean, which was considered quite satisfactory.

The effects of ice thickness and urea concentration on the elastic modulus of urea-doped ice during freeze-up are presented in Figures 23 and 24. Figure

16

Table 4. Results of systematic measurements of ice bending strength.

Date and time	Local mean strength (kPa)	Local strength deviation (kPa)	Local coef. of variation (%)	Overall mean strength (kPa)	Overall strength deviation (kPa)	Overall coef. of variation (%)
	99.6	6.5	6.5			
8 July, 1300	88.1	4.0	4.5	90.7	6.4	7.1
	84.5	3.8	4.5			
	83.8	2.7	3.2			
9 July, 0800	81.1	7.1	8.8	86.7	6.2	7.1
	95.3	9.2	9.6			
	57.1	2.1	3.6			
9 July, 1600	72.4	4.3	5.9	69.7	9.4	13.5
	79.6	3.7	4.6			
	181.0	8.8	4.9			
30 Aug, 0930	174.0	7.5	4.3	173.3	6.6	3.8
	165.0	12.1	7.3			
	200.0	11.9	5.9			
30 Aug, 1900	200.0	11.0	5.5	193.4	9.3	4.8
	180.3	15.0	8.3			
	167.5	13.7	8.2			
31 Aug, 0845	170.5	8.9	5.2	167.1	3.0	1.8
	163.2	1.8	1.1			
	148.2	10.8	7.3			
31 Aug, 1700	143.3	2.5	1.7	145.3	2.1	1.4
	144.5	11.2	7.7			
	99.5	2.9	3.0			
31 Aug, 2230	101.6	4.3	4.2	100.6	0.85	0.8
	100.6	1.6	1.6			
	75.2	2.8	3.8			
1 Sept, 0830	69.8	5.0	7.2	71.3	2.8	3.9
	69.0	3.3	4.8			
	60.9	1.6	2.6			
1 Sept, 1530	60.4	2.6	4.3	59.0	2.3	4.0
	55.7	6.1	10.9			
1 Sept, 2230	51.9	2.0	3.8	52.6	0.7	1.2
	53.2	3.6	6.7			
	48.1	1.0	2.0			
2 Sept, 0840	35.8	19.4	54.2	44.5	6.2	13.9
	49.6	5.1	10.3			
	140.9	11.4	8.1			
6 Sept, 1015	132.6	8.6	6.5	137.7	3.7	2.7
	139.7	5.1	3.6			
	148.6	4.0	2.7			
6 Sept, 1800	124.7	12.3	9.9	133.8	10.6	7.9
	128.0	5.1	4.0			
	106.8	14.7	13.8			
7 Sept, 1630	101.0	10.0	9.9	101.0	4.7	4.7
	95.2	7.9	8.3			
	75.6	1.7	2.3			
7 Sept, 2200	80.3	1.6	2.0	77.2	2.2	2.8
	75.8	1.4	1.8			
	44.7	3.6	8.0			
8 Sept, 0830	40.5	6.0	14.8	43.3	2.0	4.6
	44.8	5.9	13.1			

Date and time	Local mean strength (kPa)	Local strength deviation (kPa)	Local coef. of variation (%)	Overall mean strength (kPa)	Overall strength deviation (kPa)	Overall coef. of variation (%)
10 Sept, 2130	118.5	2.6	2.2			
	85.0	11.9	14.0	102.2	13.7	13.4
	103.0	10.0	9.7			
11 Sept, 0900	126.1	9.0	7.1			
	118.2	9.5	8.0	125.0	5.2	4.1
	130.7	3.4	2.6			
11 Sept, 1230	105.1	3.0	2.9			
	91.1	4.6	5.3	98.9	5.8	5.9
	100.6	5.7	5.6			
11 Sept, 1700	75.6	3.5	4.6			
	67.4	9.7	14.3	71.8	3.4	4.7
	72.5	2.5	3.5			
12 Sept, 0930	40.4	4.3	10.6			
	29.0	2.1	7.1˙	32.0	6.0	18.7
	26.7	2.8	10.4			
12 Sept, 1945	28.3	3.0	10.4			
	30.8	1.6	5.2	28.8	1.5	5.1
	27.3	1.5	5.4			
15 Sept, 0930	81.3	8.7	10.6			
	88.8	2.8	3.2	87.1	4.2	4.8
	91.2	9.8	10.7			
15 Sept, 1145	59.6	14.7	24.7			
	62.8	2.4	3.8	62.3	2.0	3.2
	64.4	2.4	3.7			
15 Sept, 1715	37.3	2.6	7.0			
	38.0	7.5	19.8	38.1	0.74	1.9
	39.1	5.9	15.0			
15 Sept, 2400	23.4	4.9	20.7			
	20.4	1.6	8.0	22.8	1.7	7.6
	24.5	3.3	13.4			
16 Sept, 0930	17.9	0.7	3.8			
	14.2	1.6	11.2	15.6	1.6	10.4
	14.8	2.1	14.1			
20 Sept, 0815	61.8	3.6	5.8			
	69.6	3.6	5.2	65.1	3.3	5.1
	63.9	3.9	6.1			
20 Sept, 1430	46.2	4.3	9.2			
	42.5	4.8	11.3	42.5	3.0	7.1
	38.8	3.2	8.3			
20 Sept, 2200	29.0	4.0	13.7			
	28.6	5.2	18.0	30.5	2.5	8.0
	34.0	4.6	13.4			
21 Sept, 0930	13.5	2.9	21.5			
	17.7	1.3	7.4	13.7	3.2	23.3
	9.9	0.9	8.9			
27 Sept, 0900	67.5	3.6	5.3			
	62.4	2.0	3.3	66.5	3.1	4.6
	69.7	5.9	8.5			
27 Sept, 1345	39.7	11.4	28.7	41.6	1.9	4.6
	43.5	5.5	12.7			
27 Sept, 1815	21.8	2.7	12.2	22.6	0.8	3.3
	23.3	2.3	9.7			

Date and time	Local mean strength (kPa)	Local strength deviation (kPa)	Local coef. of variation (kPa)	Overall mean strength (kPa)	Overall strength deviation (kPa)	Overall coef. of variation (kPa)
	80.6	4.7	5.9			
7 Oct, 1300	74.3	3.7	5.0	76.4	3.0	3.9
	74.3	1.2	1.6			
	127.0	7.4	5.8			
8 Oct, 0850	124.6	12.0	9.6	122.5	4.8	3.9
	115.8	6.6	6.6			
	10.4	2.2	2.4			
8 Oct, 1230	94.7	1.6	9.6	89.9	4.2	4.6
	84.5	6.1	6.6			
	58.8	3.6	6.1			
8 Oct, 1730	60.1	0.5	0.8	61.5	3.0	4.8
	65.6	4.2	6.5			
	105.2	14.5	13.8			
9 Oct, 0945	98.4	4.7	4.8	101.0	3.0	3.0
	99.3	6.9	6.9			
	66.5	3.1	4.7			
10 Oct, 0915	76.8	2.5	3.2	70.8	4.4	6.2
	69.1	1.8	2.6			
	50.8	6.3	12.3			
11 Oct, 1145	42.5	2.1	4.9	46.7	4.15	8.9
	86.9	7.0	8.1			
17 Oct, 2120	91.5	21.1	23.6	81.6	10.9	13.3
	66.5	3.2	4.9			
	115.0	8.3	7.3			
18 Oct, 1410	99.2	3.6	3.6	106.9	6.4	6.0
	106.6	4.4	4.2			
	104.6	8.2	7.8			
19 Oct, 1650	96.3	6.9	7.2	96.5	6.6	6.8
	88.5	3.2	3.6			
	63.6	7.9	12.4			
20 Oct, 0845	52.0	8.1	15.5	55.4	5.8	10.5
	50.7	5.0	9.8			
	49.2	3.9	7.9			
20 Oct, 1545	46.1	2.5	5.4	47.2	1.4	3.0
	46.3	8.8	19.1			
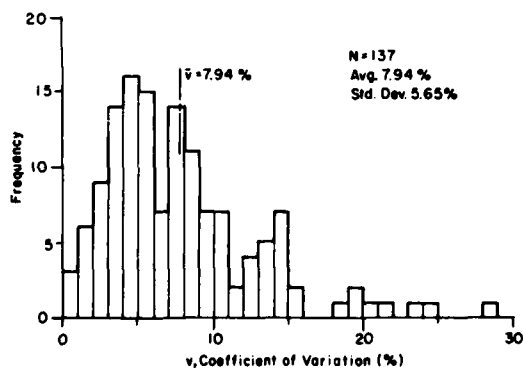
Figure 20. Local coefficient of variation of flexural strength.
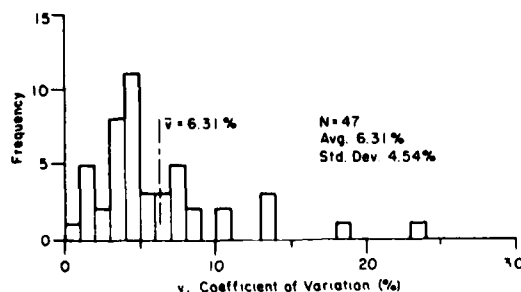
Figure 21. Overall coefficient of variation of flexural strength.

19

(m)	34	32	30	28	26	24	22	20	18	16	14	12	10	8	6	4	2	0

(MPa) 52.4 56.8 59.3 52.7 63.1 45.5 53.6 59.5 53.8

52.0 58.2 58.6 62.9 57.8 44.8 53.0 51.3 50.4
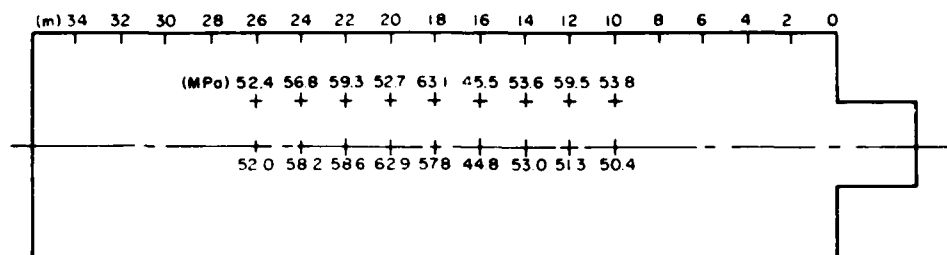
Figure 22. Distribution of elastic modulus in the tank (22 Nov 1981).
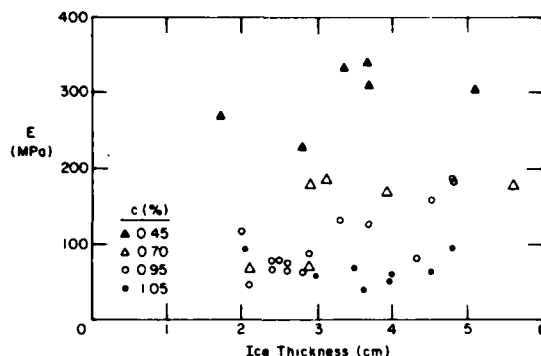
Figure 23. Effect of ice thickness on elastic modulus.

Figure 24. Effect of urea concentration on elastic modulus.

23 shows that, except for the results for thin ice sheets (of thickness of 2 to 2.5 cm) where the loads which can be applied are very small and accuracy in the measurements is questionable, the elastic modulus is practically independent of ice thickness. On the other hand, the elastic modulus decreases rapidly with increasing urea concentration from about 300 MPa at $c = 0.45\%$ to approximately 70 MPa at $c = 1.05\%$.

Finally, as shown in Figure 25, which includes measurements taken during freeze-up and warm-up of the ice sheets, the elastic modulus was found to be independent of the direction (upward or downward) of load application.

Because of insufficient data, the effect of temperature, if any, on the elastic modulus could not be investigated with any degree of confidence.

Ratio E/σ

The value of E, elastic modulus, is plotted against σ, the flexural strength in the downward mode of load application, in Figure 26. All the data are seen to lie between the two lines $E/\sigma = 500$ and $E/\sigma = 2000$. The ratio E/σ itself was plotted versus urea concentration c in Figure 27. Figure 27 indicates that E/σ decreases with urea concentration but appears to approach a constant value of about 1000 for c equal to 0.90% or more. The average values of E/σ are

Figure 25. Effect of loading direction on elastic modulus.

$E/\sigma = 1800 \pm 300$ for $c = 0.45\%$

$E/\sigma = 1250 \pm 350$ for $c = 0.70\%$

$E/\sigma = 1000 \pm 250$ for $c = 0.95\%$

$E/\sigma = 970 \pm 300$ for $c = 1.05\%$

20

Figure 26. Plot of E vs σ during freeze-up.

Figure 27. Variation of E/σ with urea concentration.
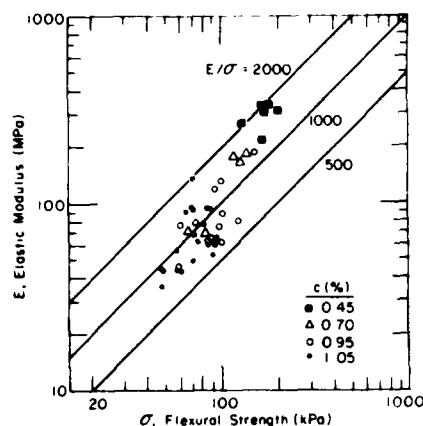
The decrease of E/σ with increasing solute concentration in the meltwater was also observed for saline ice (Schwarz 1975), and predicted analytically by Weeks and Assur (1967), who derived a relationship between E/σ and brine volume in the ice.

Finally, in Figure 28 the ratio E/σ is plotted against h_t/h. In spite of the scatter in the data points, it can be seen that E/σ generally increases with increasing h_t/h, at least in the range of this latter parameter for the present study. This variation of E/σ with h_t/h is in qualitative agreement with the two-layer model prediction as illustrated by the curve drawn in Figure 28 which corresponds to eq 19 with arbitrarily selected values of $E_1/\sigma_1 = 4000$ and $E_1/E_2 = 100$. Since no ice sheet with values of h_t/h less than 0.1 was grown in the tank, verification of the reverse behavior of E/σ with h_t/h for small h_t/h was not possible. However, Timco (pers. comm.) has
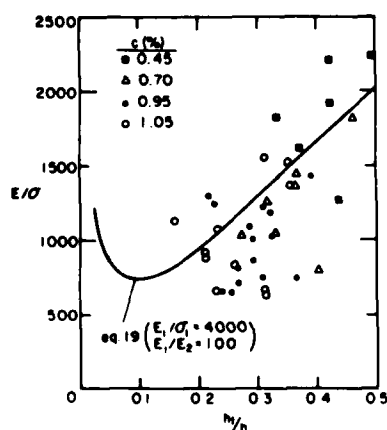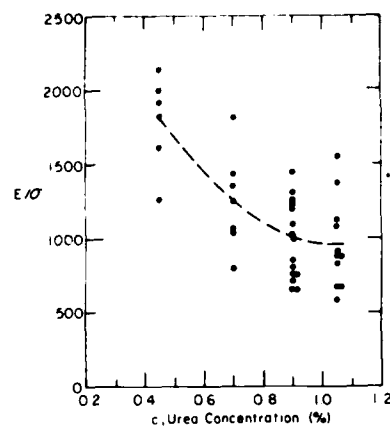
indicated that the urea-doped ice sheets grown in the test tank of the National Research Council of Canada exhibit a very thin top layer, and that values of E/σ of 1500 to 2000 were commonly measured. It is likely that the difference in top layer thickness between the two tanks is due to a difference in growth rate (higher in the NRC tank where cold air is blown over the tank).

Properties of urea-doped ice during warm-up

As mentioned in the *Introduction*, tempering of the ice sheet is the practical method for achieving the flexural strength values required in most model tests, which are usually lower than those obtained during freeze-up.

As soon as the refrigeration system in the tank room is shut off, the air temperature rises naturally, as shown in Figure 29, with corresponding variation in the ice properties, as follows.

Flexural strength

As the air temperature in the room rises, so does the ice surface temperature; consequently the strength of the sheet's top layer and, therefore, the nominal strength of the ice sheet, decreases. Additional decreases in the ice strength can be related to enlargement of the brine pockets in both the top and bottom layers. As previously mentioned, Weeks and Assur (1967) showed that the strength of sea ice decreases with brine volume, which itself increases with surrounding air temperature.

Examples of strength variation with time are shown in Figure 30 for three ice sheets grown from the same 0.95% urea solution and with nearly identical thicknesses and initial strength at the start of the warm-up period. The final strength for the tests was targeted to 20 kPa.

Figure 28. Variation of E/σ with relative top layer thickness h_t/h.

21
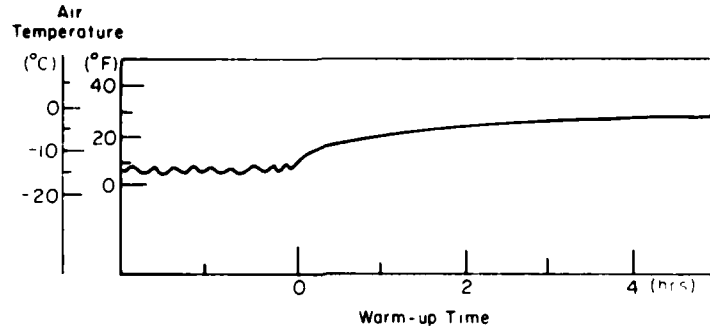
Figure 29. Example of air temperature change during warm-up.
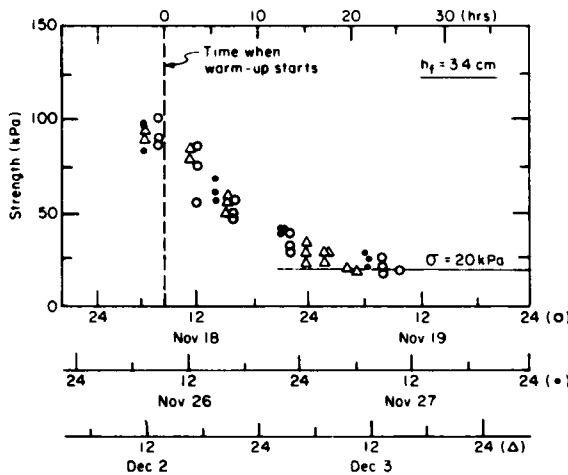
Figure 30. Examples of decrease in flexural strength during warm-up.
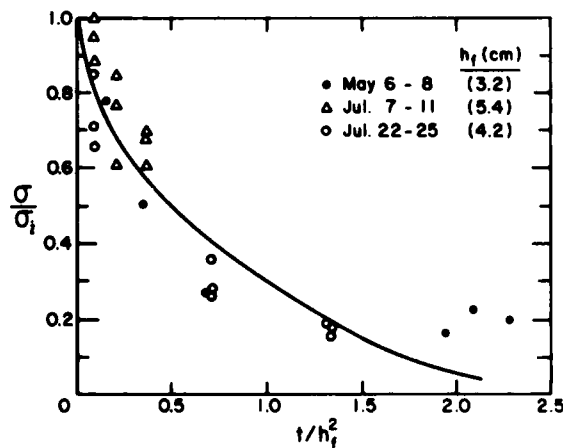
In Figure 31, the data collected for the ice sheets grown for the four urea concentrations investigated are presented as σ/σ_i versus t/h_f^2, where σ is the nominal ice strength at time t during warm-up, σ_i is the initial strength at $t = 0$, and h_f is the final desired ice thickness. The parameter t/h_i^2, where h_i is the ice thickness at the start of warm-up, $t = 0$, could also have been used since it was noted that, for the range of experimental conditions studied here, h_i and h_f are proportional to each other (see Fig. 8).

	h_f (cm)			h_f (cm)
▲ Sep 26-28	(3.1)		▫ Nov 19-23 (No.3)(5.6)	
△ Oct 6-12	(5.1)		▽ Nov 25-27 (No.4)(3.4)	
○ Oct 16-21	(5.0)		◐ Nov 27-Dec 1(No.5)(5.6)	
● Nov 12-16 (No.1)(5.6)			▼ Dec 1-3 (No.6)(3.4)	
■ Nov 17-19 (No.2)(3.3)				

a. c = 1.05%
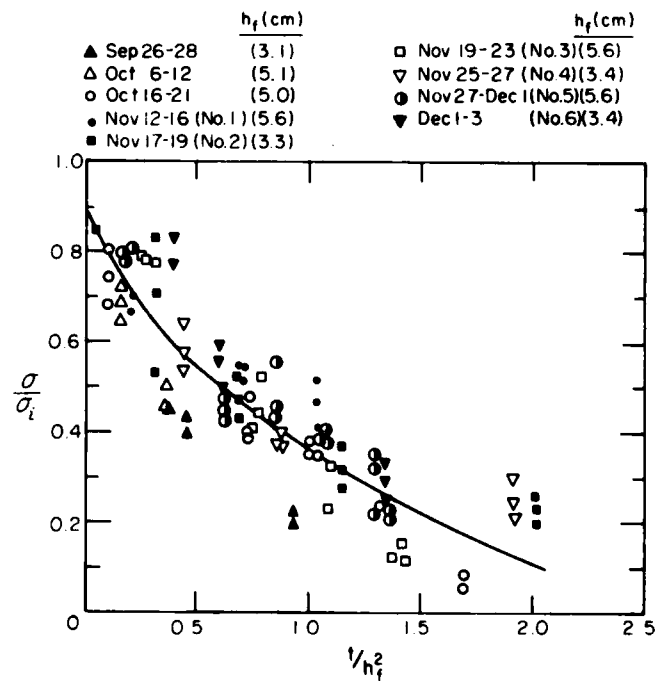
b. c = 0.95%

Figure 31. Plot of σ/σ_i vs t/h_f^2.

22
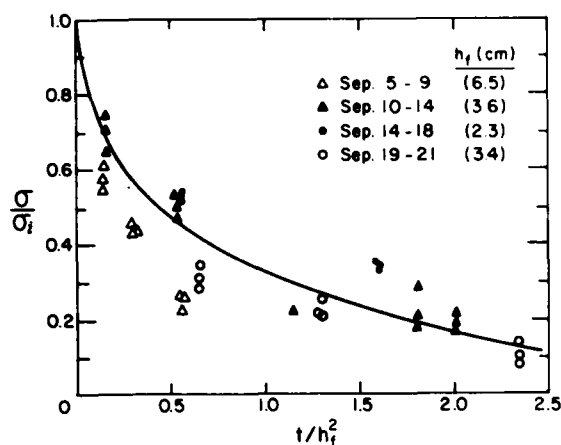
c. c = 0.70%.
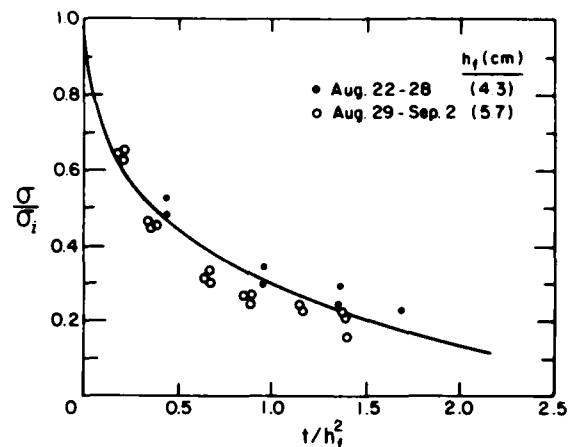
d. c = 0.45%.

Figure 31 (cont'd).
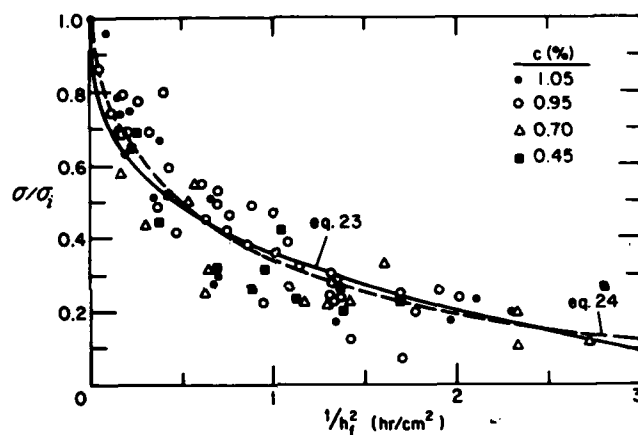
Figure 32. Plot of σ/σ_i vs t/h_f^2 for all urea concentrations.

In Figure 31, which shows that the data for each urea concentration collapse reasonably well, empirical relations of the form

$$\frac{\sigma}{\sigma_i} = 1 - p \, (t/h_f^2)^q$$

have been determined by nonlinear regression analysis, namely

$c = 1.05\%$ $\sigma/\sigma_i = 1 - 0.70 \, (t/h_f^2)^{0.48}$ (22a)

$c = 0.95\%$ $\sigma/\sigma_i = 1 - 0.64 \, (t/h_f^2)^{0.50}$ (22b)

$c = 0.70\%$ $\sigma/\sigma_i = 1 - 0.67 \, (t/h_f^2)^{0.33}$ (22c)

$c = 0.45\%$ $\sigma/\sigma_i = 1 - 0.70 \, (t/h_f^2)^{0.33}$ (22d)

The data for the four urea concentrations have been collected on the single plot shown in Figure 32, from which the following empirical relations have been calculated:

$$\frac{\sigma}{\sigma_i} = 1 - (0.25 \, t/h_f^2)^{0.33} \qquad (23)$$

and

$$\frac{\sigma}{\sigma_i} = \exp \left[- (1.12 \, t/h_f^2)^{0.63} \right] \qquad (24)$$

In eq 24 the factor $K = 1.12$ cm^2/hr might be related to the thermal diffusivity of the urea-doped ice. From Figure 32, it can be seen that eq 23 is a good approximation to eq 24 for the range $0 < t/h_f^2 < 3$.

23
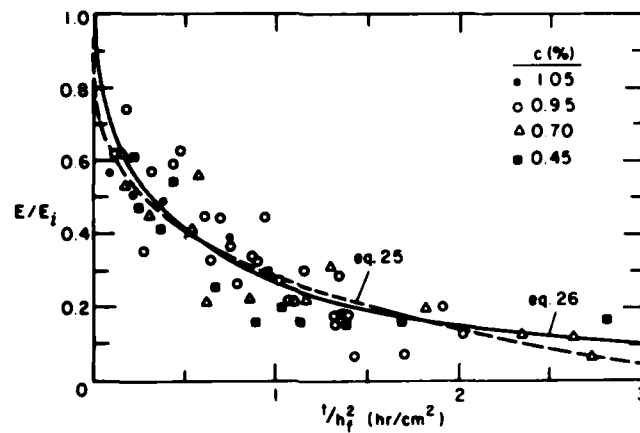
Figure 33. Plot of E/E_i vs t/h_f^2 for all urea concentrations.

Elastic modulus

The ratio E/E_i, where E_i is the elastic modulus at the start of warm-up, has been plotted against t/h_f^2 in Figure 33 for all four urea concentrations.

Two empirical relationships have been determined by nonlinear regression analysis:

$$\frac{E}{E_i} = 1 - (0.28 \; t/h_f^2)^{0.27} \tag{25}$$

and

$$\frac{E}{E_i} = \exp\left[-(1.63 \; t/h_f^2)^{0.54}\right] . \tag{26}$$

These two relationships have also been plotted in Figure 33.

Ratio E/σ

Comparison of Figures 32 and 33 indicates that the elastic modulus E decays slightly faster than the flexural strength σ with time during warm-up. Therefore, some decrease in the ratio E/σ may be expected during warm-up. However, because of the experimental scatter in the data for both σ and E, even larger scatter may be expected in their ratio. The quantity $E^* = (E/\sigma)/(E_i/\sigma_i)$ has been plotted versus t/h_f^2 in Figure 34. It can be seen that 40 out of 49 points, or 80% of the data, falll between $E^* = 0.55$ and 1.20, and that the rather considerable scatter in the data points does not allow identification of any significant variation of E^* with t/h_f^2.

The measurements of E and σ are also collected in Figure 35 as E versus σ for the four urea concentrations used in the study. From these figures it appears that the majority of the data fall between the lines $E/\sigma = 500$ and $E/\sigma = 1500$, and that the ratio E/σ generally decreases with increasing urea concentration, as mentioned previously.
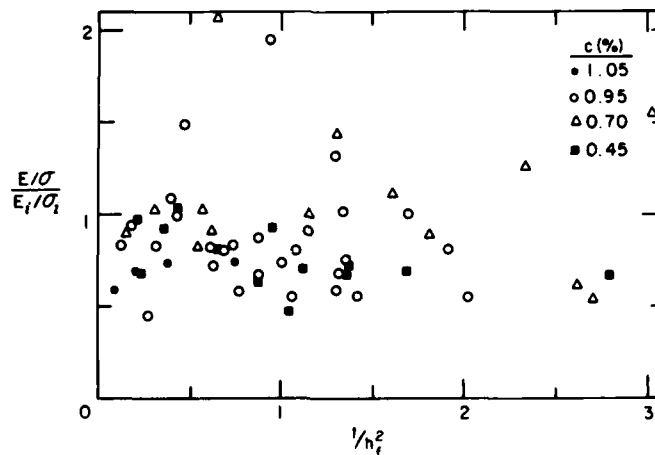
Figure 34. Plot of $(E/\sigma)/(E_i/\sigma_i)$ vs t/h_f^2.

24

Figure 35. Plot of E vs σ.

a. c = 1.05%.

b. c = 0.95%.

c. c = 0.70%.

d. c = 0.45%.

In figure a (c = 1.05%): E, Elastic Modulus (MPa) vs σ, Flexural Strength (kPa). Lines labeled $\frac{E}{\sigma} = 1500$, 1000, 500.

In figure b (c = 0.95%): E, Elastic Modulus (MPa) vs σ, Flexural Strength (kPa). Lines labeled $\frac{E}{\sigma} = 1500$, 1000, 500. Legend with h(cm):
Sep 26-28 ...
Oct 6-12 ...
Oct 16-2. (5.0)
Nov 12-16 (5.6)
Nov 17-19 (3.3)
Nov 19-23 (5.6)
Nov 25-27 (3.4)
Nov 27-Dec 1 (5.6)
Dec 1-3 (3.4)

In figure c (c = 0.70%): E, Elastic Modulus (MPa) vs σ, Flexural Strength (kPa). Lines labeled $\frac{E}{\sigma} = 2000$, 1500, 1000, 500. Legend with h(cm):
Sep 5-9 (6.4)
Sep 10-14 (3.5)
Sep 14-16 (2.2)
Sep 19-21 (3.3)

In figure d (c = 0.45%): E, Elastic Modulus (MPa) vs σ, Flexural Strength (kPa). Lines labeled $\frac{E}{\sigma} = 2000$, 1500, 1000. Legend:
Aug 22-28 (h = 4.5 cm)
Aug 29-Sep 2 (h = 6.0 cm)

APPLICATIONS TO TEST PROGRAM SCHEDULING

Any test of mechanical structures in level ice can be conducted only when the required ice characteristics, namely thickness and flexural strength, are achieved in the tank; in other words the ice controls the time at which model tests are performed. The results of the present study have been used to formulate a reliable time schedule for growing and tempering an ice sheet to reach present conditions, so that tests can be started in the morning at regular working hours rather than at odd hours of the day or night.

The method detailed below is valid for the 0.95% urea concentration now being used in the CRREL test basin, and for the particular refrigeration capabilities of the CRREL plant.

From eq 20b, 22b and 6 a family of curves have been plotted in Figure 36 for a wide range of ice thicknesses, flexural strengths, and warm-up times. When the flexural strength and ice thickness are given as test conditions to be achieved in the tank, the corresponding initial ice thickness and necessary warm-up time can be determined from Figure 36. Once the initial ice thickness is determined, the necessary freeze-up time and temperature are obtained from Figure 37, where eq 4 has been plotted as h_i versus time for several air temperatures, with the values of the coefficients k_i and h_{ia} obtained from Figure 6b. For example, to obtain a model ice sheet of final thickness h_f = 4.5 cm and final flexural strength σ = 50 kPa, Figure 36 indicates that warm-up should be started when the ice thickness reaches a value h_i = 3.9 cm and should last for approximately 18 hours.

25
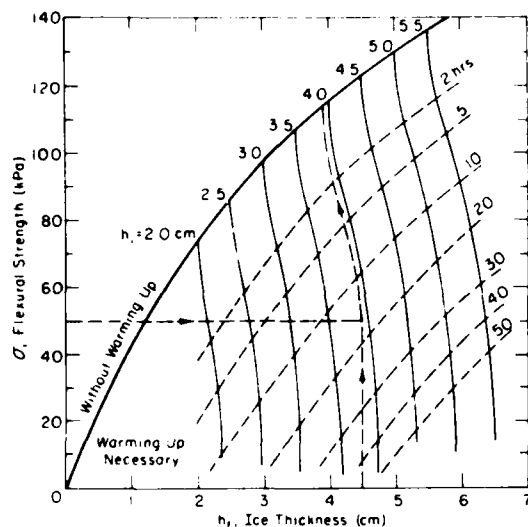
Figure 36. Diagram for planning model ice prep-
aration (c = 0.95%).

Figure 37. Expected ice thickness vs freeze-up
time for different air temperatures.

Then from Figure 37, the freeze-up time required
to grow a 3.9-cm-thick ice sheet is determined as 22
hours at an air temperature of -18°C (0°F) or 32
hours at an air temperature of -12°C (10°F).

Once the total time (freeze-up and warm-up) to
achieve required ice conditions has been determined,
either the time at which seeding should take place
can be decided, or the time at which the test is likely
to be performed can be calculated with a good degree
of confidence. In the above example, the total time
(assuming a -12°C air temperature during freeze-up)
is 50 hours. Therefore, if the test is scheduled for a
Monday morning at 0800 hours, the tank should be
seeded the preceding Saturday morning at about 0600
hours. On the other hand, if for some reason seeding
cannot be done before 1200 hours on Saturday, the
start of the test can be scheduled for Monday after-
noon at about 1400 hours, unless the air temperature
in the room during freeze-up can be adjusted to -15°C,
in which case the test is likely to be possible in the
early morning.

This scheduling method has been in operation
now for some time at CRREL and has proven to be
reliable. For example, the tests whose results are
shown in Figure 30 were so scheduled.

It goes without saying that although this method
can and does reduce the time uncertainty in sched-
uling tests in ice, monitoring of air temperature and
ice characteristics (thickness and strength) remains
necessary, but usually less frequently, to account
for any variation in plant operation or outside air
temperature, and to allow for unforeseen circum-
stances.

SUMMARY AND CONCLUSIONS

A study of the growth process and mechanical
properties of some 50 urea-doped ice sheets in the
CRREL ice test basin has led to the following results:

1. Uniformity of ice thickness in the main test
area of the basin is considered satisfactory, with a
standard deviation in the ice thickness of 1 mm or
less for thicknesses of 2 to 7 cm.

2. A relationship between ice thickness and neg-
ative degree-hours was well established.

3. The structure of urea-doped ice was found to
be similar to that of sea ice except for a relatively
thick top layer over a bottom layer of columnar
structure typical of dendritic growth.

4. A mathematical two-layer ice model was de-
veloped to predict the behavior of ice properties for
comparison with the results of laboratory measure-
ments. There is qualitative agreement between theory
and experiments. Before the mathematical two-layer
model can be improved, better understanding of the
growth mechanism of the top ice layer is necessary.

5. Uniformity of ice flexural strength and elastic
modulus in the tank was found to be satisfactory.

6. Empirical formulas were obtained that give the
relationships between 1) ice thickness, flexural strength
and elastic modulus and 2) air temperature, urea con-
centration, and ratio of top layer thickness to total
ice thickness during the freeze-up period.

7. During the tempering or warm-up period, the
reduction in strength and in elastic modulus, and the
increase in ice thickness, were quantified, and em-
pirical relationships were established.

26

8. The ratio E/σ was found to vary widely during both freeze-up and warm-up from one ice sheet to another grown under similar conditions. On the average, this ratio could be larger than 2000 for ice sheets grown from a 0.45% urea solution in water, and smaller than 1000 for ice sheets grown from a 1.05% solution. The two-layer model prediction that a considerable increase in E/σ could be achieved with ice sheets with a thin top layer (less than 5% of the total thickness) could not be verified.

9. The results of the study were combined into charts that permit establishment of a reliable test schedule for producing, in the tank, ice sheets with the required thickness and flexural strength. These charts have been used successfully.

In addition to the above results, the study has confirmed that urea-doped ice is a very satisfactory alternative to saline ice as model ice for testing ice-structure interaction. Urea-doped ice allows a model scale as low as 1/40, and practically eliminates corrosion problems in experimental facility equipment.

The study has also led to improvements in the operation of the ice tank at CRREL, and has indicated what further modifications and improvements are necessary or would be useful. In particular, measurement techniques for both flexural strength and elastic modulus could be improved, and application of different techniques would be useful for comparison between laboratory and field data. Further research efforts are needed to clarify the growth process of urea ice and its two-layer structure, in order to be able to control the thickness of the top layer and achieve as high values of the ratio E/σ as possible.

LITERATURE CITED

Afanas'ev, V.P., IU.V. Dolgopolov and Z.I. Shraysh-teyn (1972) Ice pressure on separate supporting structures in the sea. U.S. Army Cold Regions Research and Engineering Laboratory, Draft Translation 346.

Ashton, G.D. (1978) River ice. *Annual Review of Fluid Mechanics,* **10**: 369-392.

Assur, A. and W.F. Weeks (1964) Growth, structure and strength of sea ice. U.S. Army Cold Regions Research and Engineering Laboratory, Research Report 135.

Calkins, D. (1979) Accelerated ice growth in rivers. U.S. Army Cold Regions Research and Engineering Laboratory, CRREL Report 79-14.

Chalmers, B. (1958) Growth of crystals of pure materials and of the solvents. *Proceedings of the International Conference on Crystal Growth,* pp. 291-309.

Danys, J.V. and F.G. Bercha (1976) Investigation of ice forces on a conical offshore structure. *Ocean Engineering,* **5**(5): 299-310.

Edwards, R.Y., Jr. (1979) Modeling the interaction between ice and ship. IUTAM Symposium on Physics and Mechanics of Ice, Copenhagen.

Enkvist, E. (1972) On the ice resistance encountered by ships operating in the continuous mode of ice breaking. The Swedish Academy of Engineering Sciences in Finland, Report No. 24.

Frankenstein, G.E. (1979) Experience gained by use of extensive ice laboratory facilities in solving ice problems. IUTAM Symposium on Physics and Mechanics of Ice, Copenhagen.

IAHR Working Group on Ice Problems (1980) Standardization of testing methods for ice properties. *Journal of Hydraulic Research,* **18**(2): 153-165.

Lewis, J.W. (1980) Methodology to measure elastic modulus. ARCTEC, Inc., Columbia, Maryland.

Michel, B. (1978) *Ice Mechanics.* Quebec: Laval University Press.

Nevel, D. (1970) Concentrated loads on plates. U.S. Army Cold Regions Research and Engineering Laboratory, Research Report 265.

Nevel, D. (1977) Ice-breaker simulation. U.S. Army Cold Regions Research and Engineering Laboratory, CRREL Report 77-16.

Ralston, T.D. (1977) Ice force design considerations for conical offshore structures. *Proceedings, 4th International POAC Conference,* pp. 741-752.

Sandell, D.A. (1981) Carbamide ice growth in a large test basin. *Proceedings, IAHR 6th International Symposium on Ice Problems,* Quebec, pp. 367-368.

Schwarz, J. (1972) On the time dependent temperature variation within ice sheets. *Proceedings, IAHR Ice Symposium,* Leningrad, pp. 262-269.

Schwarz, J. (1975) On the flexural strength and elasticity of saline ice. *Proceedings, IAHR 3rd International Symposium on Ice Problems,* Hanover, New Hampshire, pp. 373-386.

Schwarz, J. (1977) New developments in modeling ice problems. *Proceedings, 4th International POAC Conference,* pp. 45-61.

Schwarz, J. and T. Miloh (1972) On the time dependent temperature variation within ice sheets. *Proceedings, IAHR Ice Symposium,* Leningrad, Vol. 2, pp. 262-269.

Sodhi, D., K. Kato, D. Haynes and K. Hirayama (in press) Measurement of characteristic length of model ice sheets. *Cold Regions Science and Technology.*

Tatinclaux, J.C. and K. Hirayama (1982) Determination of the flexural strength and elastic modulus of ice from in-situ cantilever beam tests. *Cold Regions Science and Technology,* **6**: 37-47.

Tiller, W.A. (1958) Alloy crystal growth. *Proceedings of International Conference on Crystal Growth*, pp. 332–341.

Timco, G.W. (1979) The mechanical and morphological properties of doped ice: A search for a better structurally simulated ice for model test basins. *Proceedings, 5th International POAC Conference*, pp. 719–739.

Timco, G.W. (1980) The mechanical properties of saline-doped and carbamide urea-doped model ice. *Cold Regions Science and Technology*, 3: 45–56.

Timco, G.W. (1981) Flexural strength of ice grown from chemically impure melts. *Cold Regions Science and Technology*, 4: 81–92.

Timco, G.W. (1981) On the test method for model ice. *Cold Regions Science and Technology*, 4.

Timco, G.W. and R.M.W. Frederking (1981) Comparative strength of freshwater ice. National Research Council of Canada, Ottawa, Canada.

Timoshenko, S. and J.N. Goodier (1951) *Theory of Elasticity*. New York: McGraw-Hill.

Tryde, P. (1977) Intermittent ice forces acting on inclined wedges. U.S. Army Cold Regions Research and Engineering Laboratory, CRREL Report 77-26.

Weast, R.C. (1973) *Handbook of Chemistry and Physics*, 53rd Edition. CRC Press.

Weeks, W.F. and A. Assur (1967) Mechanical properties of sea ice. U.S. Army Cold Regions Research and Engineering Laboratory, Monograph II-C3.

Yean, J.S., J.C. Tatinclaux and A.G. Cook (1981) Ice forces on two-dimensional sloping structures. IIHR Report No. 230, Institute of Hydraulic Research, University of Iowa, Iowa City, Iowa.

Yen, Y.C. (1981) Review of thermal properties of snow, ice and sea ice. U.S. Army Cold Regions Research and Engineering Laboratory, CRREL Report 81-10.

APPENDIX A: RESULTS OF ICE THICKNESS MEASUREMENTS FOR VARIOUS GROWTH CONDITIONS

Experiment period	Time after seeding (hr)	Total thickness (cm)	Top layer thickness (cm)	$\Sigma°C \times hr$
20 - 22 Apr	5.0	0.62	0.20	-43.3
	21.0	1.95	0.55	-180.5
	27.0	2.55	0.65	-232.5
	30.5	2.75	0.70	-262.5
	45.0	3.85	0.82	-389.5
23 - 24 Apr	1.0	0.2		
	4.0	0.50	0.17	-41.0
	9.0	0.95	0.30	-92.5
	24.0	2.43	0.67	-25.1
24 - 27 Apr	4.0	0.5	0.1	-47.5
	18.5	2.1	0.65	-203.5
	27.0	3.4	0.65	-302.5
	66.0	6.8	0.90	-745.5
28 - 30 Apr	4.0	0.50	0.14	-44.5
	21.5	2.12	0.60	-239.0
	30.0	2.29	0.84	-335.5
	45.5	4.25	1.09	-516.5
4 - 5 May	14.0	1.99	0.55	-133
	19.0	2.51	0.63	-248

Note: urea concentration c = 1.05%

Experiment period	Time after seeding (hr)	Total thickness (cm)	Top layer thickness (cm)	$\Sigma°C \times hr$
11 - 15 June	19.5	2.99	0.74	-254
	34.0	3.89	0.88	-380
	44.5	5.24	1.06	-519
	67.5	7.38	1.15	-818
17 - 19 June	4.5	0.68	0.27	-59
	20.5	2.65	0.72	-269
	27.5	3.26	0.91	-343
	44	4.82	1.03	-547
19 - 22 June	18.5	2.14	0.72	-219
	43.0	4.34	1.05	-501
	67.5	6.47	1.31	-780
24 - 26 June	5.0	0.72	0.23	-46
	20.5	2.21	0.76	-151
	29.5	3.05	1.01	-274
	44.5	4.25	1.16	-415
26 - 29 June	18.0	1.92	0.59	-172
	42.0	4.06	1.00	-416
	66.0	6.01	1.21	-667

Note: urea concentration c = 1.05%

Experiment period	Time after seeding (hr)	Total thickness (cm)	Top layer thickness (cm)	°C·x·hr
5 – 7 Sept	8.5	1.40	0.55	-114.5
(seeded 1300 5 Sept)	20.0	2.91	1.05	-275.2
	28.0	3.82	1.20	-369.5
	43.0	5.42	1.45	-576.2
10 – 11 Sept	12.5	1.61	0.74	-134.6
(seeded 0830 10 Sept)	23.5	2.85	1.04	-261.2
14 – 15 Sept	17.0	2.02	0.81	-192.5
(seeded 1515 14 Sept)				
19 – 21 Sept	17.5	2.75	0.91	-243.9
(seeded 1330 19 Sept)				
26 – 27 Sept	17.0	2.38	0.75	-201.7
(seeded 1430 26 Sept)				
6 – 8 Oct	19.0	2.35	0.75	-222.2
(seeded 1715 6 Oct)	39.0	4.25	1.03	-456.1
16 – 19 Oct	21.0	1.93	0.75	-173.3
(seeded 0030 17 Oct)	36.5	3.21	1.00	-315.9
	43.0	3.75	1.09	-373.9
	55.5	4.61	1.32	-482.5
12 – 14 Nov	12.5	1.99	0.58	-164.0
(seeded 1915 12 Nov)	21.3	3.23	0.75	-291.9
	43.0	5.15	1.00	-566.9
17 – 18 Nov	17.0	2.71	0.69	-227.2
(seeded 1440 17 Nov)				
19 – 21 Nov	14.0	1.99	0.61	-177.2
(seeded 1350 19 Nov)	21.5	2.80	0.73	-234.7
	36.5	4.92	1.07	-496.8
25 – 26 Nov	16.5	2.56	0.68	-215.7
(seeded 1500 25 Nov)				
27 – 29 Nov	15.0	1.99	0.73	-190.0
(seeded 1740 27 Nov)	24.5	2.87	0.85	-300.3
	39.0	4.42	0.99	-485.1
	42.5	4.80	1.08	-532.5
1 – 2 Dec	15.5	2.21	0.65	-222.6
(seeded 1700 1 Dec)	20.0	2.76	0.73	-293.5

Note: urea concentration c = 0.70% from 5 to 21 Sept
c = 0.95% from 26 Sept on

30

APPENDIX B: PROPERTIES OF UNTEMPERED ICE

Experiment period	Urea concentration (%)	Time of beam tests	Beam thickness (cm)	Flexural strength (kPa)	Elastic modulus (MPa)
27-29 May 1981	1.05	28 May - 0930	2.5	42.2 ± 6.1	
			2.6	45.9 ± 2.0	
		28 May - 1600	3.1	34.3 ± 0.2	
			2.9	35.1 ± 1.8	
		28 May - 2100	3.3	24.9 ± 2.3	
			3.1	39.3 ± 4.9	
		29 May - 0800	3.4	24.1 ± 2.1	
			3.5	21.9 ± 1.4	
		29 May - 1400	3.65	20.3 ± 1.3	31.6
1-3 June 1981	1.05	2 June - 0900	1.75	56.4 ± 6.4	
			1.9	58.6 ± 5.9	
			1.9	87.9 ± 16.8	
		2 June - 1600	2.4	93.2 ± 12.0	
			2.4	92.0 ± 4.6	
			2.4	66.5 ± 4.0	
		3 June - 0900	3.75	72.3 ± 4.5	
			4.1	79.2 ± 5.0	
			3.9	100 ± 12.3	
		3 June - 1030	3.9	110 ± 3.2	
			4.0	75 ± 4.1	
		3 June - 1200	4.0	87.7 ± 5.3	
			4.2	84.7 ± 8.2	
			4.1	32.8 ± 3.8	251.0
3-5 June 1981	1.05	4 June - 1030	1.85	68.4 ± 4.4	
			2.0	60.3 ± 3.9	91.7
			1.9	71.2 ± 3.1	
		4 June - 1630	2.3	80.9 ± 1.4	
			2.45	70.9 ± 4.2	
			2.4	82.9 ± 8.1	
		5 June - 0830	3.8	78.2 ± 2.3	
			3.9	89.0 ± 5.7	
			3.75	94.1 ± 10.2	
		5 June - 1100	4.0	103.4 ± 11.2	
			4.1	87.1 ± 3.3	23.2
			4.1	111.4 ± 9.6	

Experiment period	Urea concentration (%)	Time of beam tests	Beam thickness (cm)	Flexural strength (kPa)	Elastic modulus (MPa)
5-8 June 1981	1.05	6 June - 0800	1.7	47.5 ± 15.9	
			1.8	52.9 ± 2.9	
			1.9	48.8 ± 3.2	
		6 June - 2030	2.85	59.4 ± 3.8	
			2.9	69.0 ± 13.9	
			3.1	62.3 ± 1.9	
		7 June - 0900	3.75	70.7 ± 3.6	
			3.85	70.5 ± 10.4	
			4.1	58.8 ± 4.5	
		7 June - 1900	4.4	75.0 ± 5.5	
			4.6	72.6 ± 3.6	
			4.8	53.3 ± 3.2	
		8 June - 0830	5.2	94.0 ± 4.5	
		8 June - 1100	5.6	85.5 ± 6.1	
			5.4	77.3 ± 2.2	
			5.9	62.1 ± 7.8	
8-11 June 1981	1.05	10 June - 0900	2.7	81.6 ± 7.2	
			2.75	74.7 ± 7.5	
			2.85	57.7 ± 5.6	
			2.55	83.1 ± 8.1	
		10 June - 1630	3.6	76.5 ± 4.9	
			3.4	79.4 ± 7.1	62.8
			3.55	67.2 ± 3.6	
		11 June - 0830	4.7	91.9 ± 3.8	
			4.5	89.8 ± 4.6	59.8
			4.65	90.8 ± 6.9	
11-15 June 1981	1.05	13 June - 2300	4.0	48.9 ± 4.2	43.7
		14 June - 0930	5.1	88.1 ± 5.3	
		15 June - 0930	7.6	69.0 ± 5.9	
			7.65	101.7 ± 1.0	
			7.75	69.0 ± 9.8	
		15 June - 1200	7.7	152.0 ± 23.3	
			7.6	135.7 ± 8.9	16.3
17-19 June 1981	1.05	18 June - 0900	2.8	50.1 ± 4.9	
			2.85	54.6 ± 4.2	12.5
			2.7	56.3 ± 5.7	
		18 June - 1600	3.3	65.9 ± 3.3	

Experiment period	Urea concentration (%)	Time of beam tests	Beam thickness (cm)	Flexural strength (kPa)	Elastic modulus (MPa)
			3.45	58.3 ± 1.4	
			3.4	58.2 ± 3.2	
		19 June – 0900	4.9	99.6 ± 8.3	
			5.1	88.9 ± 14.3	
			5.1	90.0 ± 6.2	
			5.3	95.8 ± 7.9	
19–22 June 1981	1.05	20 June – 0800	2.1	67.7 ± 5.8	
			2.2	66.4 ± 7.0	
			2.4	70.4 ± 4.6	
		21 June – 0800	4.4	87.6 ± 3.8	
			4.5	91.4 ± 8.6	
			4.7	90.3 ± 6.0	
		22 June – 0900	6.45	92.3 ± 8.9	
			6.6	89.2 ± 8.8	
24–26 June 1981	1.05	25 June – 0830	2.2	55.5 ± 8.4	
			2.4	65.2 ± 3.9	
			2.3	68.1 ± 4.6	
		26 June – 0800	4.15	95.3 ± 4.1	
			4.25	91.8 ± 4.2	
			4.6	88.6 ± 5.4	
26–29 June 1981	1.05	27 June – 0800	1.9	55.0 ± 6.6	
			2.1	50.3 ± 6.2	
			2.0	51.5 ± 1.1	
		28 June – 0800	4.0	79.3 ± 7.0	
			4.3	81.0 ± 5.8	
			4.1	82.8 ± 3.5	
		29 June – 0800	6.25	99.5 ± 7.0	
			5.9	77.6 ± 18.3	
			6.35	92.0 ± 4.9	
		29 June – 1130	6.5	73.3 ± 1.3	
			6.2	63.4 ± 0.9	
			6.35	93.2 ± 5.2	
30 June – 1 July 1981	1.05	1 July – 0800	3.55	83.5 ± 3.2	
			3.7	87.9 ± 7.2	
			3.7	88.6 ± 6.0	
2–6 July 1981	1.05	3 July – 1130	2.3	52.6 ± 4.0	
			2.5	63.0 ± 5.0	
			2.4	58.5 ± 9.2	

Experiment period	Urea concentration (%)	Time of beam tests	Beam thickness (cm)	Flexural strength (kPa)	Elastic modulus (MPa)
		4 July – 1030	3.9	70.6 ± 2.2	
			4.4	79.5 ± 4.6	
			4.3	74.3 ± 5.3	
		5 July – 1330	6.0	94.8 ± 5.1	
			6.2	91.2 ± 27.8	
			6.2	96.9 ± 12.2	
			5.9	87.7 ± 3.2	
		6 July – 0900	7.0	105.2 + 6.8	
			7.4	139.8 ± 12.4	
			7.2	124.5 + 18.9	
		6 July – 1230	7.4	82.2 + 5.7	
			7.6	106.3 + 9.2	84.6
			7.5	96.1 + 7.5	
		6 July – 1400	7.4	83.6 + 1.6	
			7.7	78.6 + 9.2	74.0
			7.6	78.5 + 10.2	
13–15 July 1981	1.05	15 July – 0800	2.7	95.9 ± 8.0	
			2.8	83.6 ± 5.5	
			2.75	102.5 + 7.2	
		15 July – 0930	3.0	101.8 ± 4.5	
			2.85	86.4 ± 9.3	
			2.8	107.6 + 9.2	
19–21 July 1981	1.05	20 July – 0900	3.55	87.0 ± 2.6	
			3.7	79.9 ± 5.2	
			3.55	85.8 + 2.6	
		21 July – 0800	4.4	92.0 ± 2.8	
			4.4	87.5 ± 4.1	13.4
			4.6	85.1 ± 4.7	

34

APPENDIX C: PROPERTIES OF TEMPERED ICE

Exp. Period 6-8 May '81   Final ice thickness $h_f = 3.2$ cm

Concentration 1.05%

Note: Warm-up started 7 May, at 1230

Date, time	Ice thickness h(cm)	Flexural strength (kPa) σ	σ'	σ'/σ	σ/σ_l ($\sigma_l = 75.2$ kPa)	Elastic modulus (MPa) E	E'	Warm-up time t(hr)	t/h_f^2
7 May 1100	2.63 - 2.78	75.2 ± 2.6							
7 May 1400	2.96	58.5 ± 1.0			0.78			1.5	0.147
7 May 1610	3.20	38.1 ± 4.1			0.51			3.5	0.342
7 May 2130	3.25	20.8 ± 2.2			0.21			9.0	0.879
8 May 0815	3.20	12.6			0.17			20.0	1.953
8 May 1000	3.10	17.3 ± 1.0			0.23			21.5	2.100
8 May 1200	3.10	15.0 ± 1.5			0.20			23.5	2.294

Exp. Period 7-11 July '81   Final ice thickness $h_f = 5.4$ cm

Concentration 1.05%

Note: Warm-up started 9 July, at 1030

Date, time	Ice thickness h(cm)	Flexural strength (kPa) σ	σ'	σ'/σ	σ/σ_l ($\sigma_l = 84.7$ kPa)	Elastic modulus (MPa) E	E'	Warm-up time t(hr)	t/h_f^2
8 July 1300	2.9 - 2.95	99.6 ± 6.5							
	3.0	88.1 + 4.0				60			
	3.0	84.5 ± 3.8							
9 July 0800	4.8	83.8 ± 2.7							
	4.8	81.1 ± 7.1				94			
	4.65 - 4.7	95.3 ± 9.1							
9 July 1300	5.1	83.1 ± 6.1			0.89				
	5.2	89.8 ± 3.5			0.96	53		2.5	0.09
	5.2	95.1 ± 7.7			1.02				
9 July 1600	5.25	57.1 ± 2.1			0.61				
	5.4	72.4 ± 4.3			0.78	48		6	0.21
	5.3	79.6 ± 3.7			0.85				

Date, time	Ice thickness h(cm)	Flexural strength (kPa) σ	σ'	σ'/σ	σ/σ_l ($\sigma_l = 111$ kPa)	Elastic modulus (MPa) E	E'	Warm-up time t(hr)	t/h^2 f
9 July	5.45	64.8 ± 2.3		0.70					
2130	5.6	63.4 ± 2.0		0.68		45		11	0.38
	5.5	57.2 ± 5.2		0.61					
10 July	5.5	50.5 ± 3.0		0.54					
0830	5.65	47.1 ± 6.1		0.51		36		22	0.75
	5.5	45.1 ± 3.3		0.48					

Exp. Period 22-25 July '81   Final ice thickness h_f = 4.2 cm
Concentration 1.05%
Note: Warm-up started 24 July, at 1030

Date, time	Ice thickness h(cm)	Flexural strength (kPa) σ	σ'	σ'/σ	σ/σ_l (σ_l = 93.1 kPa)	Elastic modulus (MPa) E	E'	Warm-up time t(hr)	t/h^2 f
23 July	2.75	93.8 ± 5.4							
1400	2.95	78.8 ± 2.1							
	2.75	86.0 ± 3.2							
24 July	4.15	82.1 ± 5.5							
0830	4.10	70.6 ± 4.0				51			
	4.10	80.9 ± 2.9							
24 July	4.2 – 4.3	59.9 ± 4.1		0.71					
1200	4.2	56.6 ± 0.4		0.67				1.5	0.09
	4.0	72.2 ± 10.9		0.85					
24 July	4.3	30.2 ± 3.1		0.36					
2300	4.3 – 4.4	21.6 ± 4.3		0.26				12.5	0.709
	4.25	23.6 ± 6.9		0.28					
25 July	4.0	15.1 ± 2.0		0.18					
1000	4.1	13.2 ± 2.3		0.16				23.5	1.33
	4.2 – 4.3	15.3 ± 3.3		0.18					

Exp. Period 18-21 Aug '81   Final ice thickness h_f = 2.50 cm
Concentration 0.45%
Note: Warm-up started 19 Aug., at 1530.

Date, time	Ice thickness h(cm)	Flexural strength (kPa) σ	σ'	σ'/σ	σ/σ_l (σ_l = 111 kPa)	Elastic modulus (MPa) E	E'	Warm-up time t(hr)	t/h^2 f
19 Aug. 0900 – 1000	2.15	76.2 ± 10.1				408			
19 Aug. 1630 – 1700	2.45	76.7 ± 3.1	74.9 ± 1.1	0.98	0.69	192		1.5	0.24
19 Aug. 2200 – 2230	2.50	47.2 ± 6.9	32.3 ± 4.6	0.68	0.43	81		6.5	1.04

Date, time	Ice thickness h(cm)	Flexural strength (kPa) σ	σ'	σ'/σ	σ/σ$_l$ (σ$_l$ = 75.2 kPa)	Elastic modulus (MPa) E	E'	Warm-up time t(hr)	t/h^2_f
20 Aug. 0830 - 0930	2.50	28.6 ± 2.4	16.9 ± 0.8	0.59	0.26	69		17.5	2.80
20 Aug. 1430	2.50	19.2 ± 2.2	17.8 ± 1.9	0.93	0.17			23.0	3.68
21 Aug. 0500	2.50	24.7 ± 3.5			NA			(refreeze) NA	
21 Aug. 1000	2.6	36.6 ± 2.9			NA			(refreeze) NA	
	2.6	61.7 ± 2.9			NA		62		NA

Exp. Period 22-28 Aug '81   Final ice thickness h$_f$ = 4.3 cm
Concentration 0.45%
Note: Warm-up started 26 Aug., at 1515

Date, time	Ice thickness h(cm)	Flexural strength (kPa) σ	σ'	σ'/σ	σ/σ$_l$ (σ$_l$ = 226 kPa)	Elastic modulus (MPa) E	E'	Warm-up time t(hr)	t/h^2_f
25 Aug. 2015 - 2030	1.70	126.5 ± 10.2	85.2 ± 2.8	0.67		270			
26 Aug. 1100	3.25	167.1 ± 10.3	104.9 ± 2.8	0.63		337			
26 Aug. 1510	3.8	213.6 ± 18.4							
	3.56	177.2 ± 5.5	81.3 ± 6.4	0.46		340			
	3.2	220.0 ± 20.5	144.0 ± 11.3	0.65					
26 Aug. 2310	4.1	112.4 ± 9.9			0.55				
	3.96	98.6 ± 5.54	62.0 ± 5.73	0.63	0.48	185		8	0.43
27 Aug. 0845	4.3	69.95 ± 5.3	42.5 ± 12.8	0.61	0.34				
	4.20	61.6 ± 4.6	27.7 ± 2.8	0.45	0.30	102		17.5	0.95
27 Aug. 1610	4.3 - 4.4	60.6 ± 3.1	28.2 ± 2.6	0.47	0.29				
	4.29	50.5 ± 2.2	20.2 ± 1.5	0.40	0.25	64		25	1.35
27 Aug. 2200	4.3	46.8 ± 4.7	27.7 ± 5.4	0.59	0.23				
	4.35	46.7 ± 5.4	16.7 ± 2.7	0.36	0.23	53		31	1.68

Exp. Period 29 Aug - 2 Sept '81   Final ice thickness h_f = 5.7 cm
Concentration 0.45%
Note: Warm-up started 31 Aug., at 1000

Date, time	Ice thickness h(cm)	Flexural strength (kPa) σ	σ'	σ'/σ	σ/σ_j (σ_j = 225 kPa)	Elastic modulus (MPa) E	E'	Warm-up time t(hr)	t/h_f^2
30 Aug.	2.9	181.0 ± 8.8	79.8 ± 7.0	0.44					
0900 - 1005	2.80	174.0 ± 7.4	66.9 ± 7.8	0.39		220			
	2.55 - 2.60	165.0 ± 12.1	82.6 ± 10.8	0.50					
30 Aug.	3.7	199.9 ± 11.9	95.4 ± 7.0	0.48					
1830 - 1930	3.70	200.0 ± 11.0	94.4 ± 6.7	0.47		312			
	3.65	180.3 ± 15.0	82.8 ± 12.0	0.46					
31 Aug.	4.9 - 5.0	167.5 ± 13.6	107.1 ± 1.7	0.64					
0810 - 0930	5.10	170.5 ± 8.9	103.1 ± 8.9	0.60		306			
	5.1	163.2 ± 1.8	89.1 ± 4.7	0.55					
31 Aug.	5.5	148.2 ± 10.8	71.1 ± 5.6	0.48	0.65				
1630 - 1730	5.60	143.3 ± 2.5	68.3 ± 3.4	0.48	0.63	189		7	0.21
	5.5	144.5 ± 11.2	65.7 ± 5.3	0.46	0.64				
31 Aug.	5.6 - 5.65	99.5 ± 2.9	41.3 ± 1.6	0.41	0.44				
2230	5.71	101.6 ± 4.3	39.1 ± 2.4	0.39	0.45	126		12.5	0.37
	5.6	100.6 ± 1.6	38.9 ± 5.3	0.39	0.44				
1 Sept.	5.7	75.2 ± 2.8	25.5 ± 1.0	0.34	0.33				
0820	5.7 - 5.85	69.8 ± 5.0	23.6 ± 0.8	0.34	0.31	79		22.5	0.67
	5.6	69.0 ± 3.3	25.2 ± 0.9	0.36	0.30				
1 Sept.	5.75	60.9 ± 1.6	18.3 ± 2.1	0.30	0.27				
1530	5.7	60.4 ± 2.6	13.3 ± 0.3	0.32	0.27	50		29.5	0.88
	5.6 - 5.8	55.7 ± 6.1	12.0 ± 0.6	0.21	0.25				
1 Sept.	5.7 - 5.8	51.9 ± 2.0	15.8 ± 1.3	0.30	0.23				
2230	5.85	53.2 ± 3.6	12.4 ± 3.7	0.23	0.23	49		37.5	1.12
2 Sept.	5.70	48.1 ± 1.0	13.8 ± 1.0	0.28	0.21				
0840	5.75 - 5.80	35.8 ± 19.4	15.0 ± 1.4	0.42	0.16	45		46.5	1.38
	5.40	49.6 ± 5.1	11.6 ± 1.1	0.234	0.22				

Exp. Period 3 - 9 Sept '81   Final ice thickness h_f = 6.5 cm
Concentration 0.70%
Note: Warm-up started 7 Sept., at 0900

Date, time	Ice thickness h(cm)	Flexural strength (kPa) σ	σ'	σ'/σ	σ/σ_j (σ_j = 176 kPa)	Elastic modulus (MPa) E	E'	Warm-up time t(hr)	t/h_f^2
6 Sept.	3.10	140.9 ± 11.4	73.6 ± 8.8	0.52		187	176		
0930 - 1100	3.10	132.6 ± 8.6	87.0 ± 3.9	0.66					
	2.90	139.7 + 5.1	63.3 ± 5.7	0.45					
6 Sept.	3.83 - 3.90	148.6 ± 4.0	85.2 ± 3.4	0.57					
1730 - 1830	3.8 - 3.9	124.7 ± 12.3	77.7 ± 1.8	0.62		169	192		
		128.0 ± 5.1	108.1 ± 6.6	0.85					
7 Sept.									
0830 - 0850	5.6	151.9 ± 5.5				179	182		
	5.3	191.4 ± 2.2	80.3 ± 5.5	0.42					
7 Sept.	6.12 - 6.17	106.8 ± 14.7	67.75 ± 1.4	0.63	0.61				
1540 - 1700	6.3	101.0 ± 10.0	61.0 ± 0.1	0.60	0.57	95	99	7	0.17
	6.0 - 6.1	95.2 ± 7.9	62.6 ± 1.0	0.66	0.54				

Date, time	Ice thickness h(cm)	Flexural strength (kPa) σ	σ'	σ'/σ	σ/σ$_i$ (σ$_i$ = 176 kPa)	Elastic modulus (MPa) E	E'	Warm-up time t(hr)	t/h² f
7 Sept. 2130 - 2230	6.4	75.6 ± 1.7	33.4 ± 2.6	0.44	0.43				
	6.35	80.3 ± 1.6	36.0 ± 2.2	0.45	0.46	80	74	13	0.31
	6.15	75.8 ± 1.4	39.1 ± 1.2	0.52	0.43				
8 Sept. 0800 - 0900	6.5	44.7 ± 3.6	18.9 ± 0.9	0.42	0.25				
	6.50 - 6.55	40.5 ± 6.0	20.5 ± 2.8	0.51	0.23	40	43	23.5	0.62
	6.15 - 6.25	44.8 ± 5.9	17.4 ± 1.7	0.39	0.25				
8 Sept. 1640 - 1710	6.5								
	6.4					41	43	32	0.85
	6.23 - 6.25								

Exp. Period 10 - 14 Sept '81   Final ice thickness h$_f$ = 3.6 cm
Concentration 0.70%
Note: Warm-up started 11 Sept., at 1000

Date, time	Ice thickness h(cm)	Flexural strength (kPa) σ	σ'	σ'/σ	σ/σ$_i$ (σ$_i$ = 143 kPa)	Elastic modulus (MPa) E	E'	Warm-up time t(hr)	t/h² f
10 Sept. 2110 - 2200	1.75	118.5 ± 2.6	66.0 ± 2.1	0.55					
	1.65	85.0 ± 11.9	43.9 ± 3.7	0.52			186		
	1.65	10.30 ± 10.0	64.45 ± 6.9	0.63					
11 Sept. 0820 - 0940	2.9	126.1 ± 9.0	62.2 ± 3.1	0.49					
	2.9	118.2 ± 9.5	65.6 ± 6.7	0.55		180	190		
	3.0	130.7 ± 3.4	65.8 ± 2.7	0.50					
11 Sept. 1200 - 1315	3.35	105.1 ± 3.0	63.9 ± 2.2	0.61	0.73				
	3.2 - 3.6	91.1 ± 4.9	45.7 ± 3.3	0.50	0.64	111	124	2	0.16
	3.2 - 3.3	100.6 ± 5.6	62.9 ± 2.1	0.63	0.70				
11 Sept. 1630 - 1715	2.48	75.6 ± 3.5	36.4 ± 5.8	0.48	0.53				
	3.50	67.4 ± 9.7	32.8 ± 3.2	0.49	0.47	74	73	7	0.54
	3.45	72.5 ± 2.5	28.4 ± 2.4	0.39	0.51				
12 Sept. 0100	3.55	32.0 ± 1.6	11.6 ± 0.7	0.36	0.22	40		15	1.16
12 Sept. 0900 - 1020	3.55	40.4 ± 4.3	20.3 ± 1.8	0.50	0.28				
	3.6	29.0 ± 2.0	16.9 ± 1.3	0.58	0.20	35	37	23.5	1.81
	3.55	26.7 ± 2.8	15.6 ± 1.8	0.58	0.19				
12 Sept. 1900 - 2045	3.5	28.3 ± 3.0	10.1 ± 0.1	0.36	0.20				
	3.65	30.8 ± 1.6	13.2 ± 0.7	0.43	0.29	22	23	34	2.62
	3.5	27.3 ± 1.5	18.5 ± 1.1	0.68	0.19				
13 Sept. 1740	3.5	17.2 ± 0.3	13.9 ± 2.6	0.81	0.12	10		55.5	4.28

39

Exp. Period 14 - 18 Sept '81   Final ice thickness h_f = 2.3 cm
Concentration 0.70%
Note: Warm-up started 15 Sept., at 0830

Date, time	Ice thickness h(cm)	Flexural strength (kPa) σ	σ'	σ'/σ	σ/σ_l (σ_l = 114 kPa)	Elastic modulus (MPa) E	E'	Warm-up time t(hr)	t/h^2 f
15 Sept.	2.10	81.3 ± 8.7	46.0 ± 5.6	0.57	0.71				
0900 - 0950	2.05	88.8 ± 2.8	47.2 ± 5.2	0.53	0.78	69		0.5	0.09
	2.00	91.2 ± 9.8	57.9 ± 0.7	0.64	0.80				
15 Sept.	2.2	59.6 ± 14.7	47.0 ± 3.0	0.79	0.52				
1120 - 1215	2.2	62.8 ± 2.4	44.3 ± 3.3	0.70	0.55	39		3	0.57
	2.1	64.4 ± 2.4	40.1 ± 4.4	0.62	0.57				
15 Sept.	2.3	37.3 ± 2.6	25.7	0.69	0.33				
1700 - 1730	2.25	38.0 ± 7.5	28.7 ± 2.1	0.76	0.33	26		8.5	1.61
	2.16 - 2.18	39.1 ± 5.9	26.4 ± 5.7	0.68	0.34				
15 Sept.	2.3	23.4 ± 4.9	21.5 ± 1.2	0.92	0.21				
2400 - 0040	2.3	20.4 ± 1.6	15.9 ± 0.1	0.78	0.18	22		16	3.03
	2.15	24.5 ± 3.3			0.21				
16 Sept.	2.2 - 2.3	17.9 ± 0.7	16.3 ± 1.1	0.91	0.16				
0900 - 1010	2.2	14.2 ± 1.6	14.7 ± 2.4	1.04	0.12	20		25	4.73
	2.1	14.8 ± 2.1			0.13				

Exp. Period 19 - 21 Sept '81   Final ice thickness h_f = 3.4 cm
Concentration 0.70%
Note: Warm-up started 20 Sept., at 0700

Date, time	Ice thickness h(cm)	Flexural strength (kPa) σ	σ'	σ'/σ	σ/σ_l (σ_l = 136 kPa)	Elastic modulus (MPa) E	E'	Warm-up time t(hr)	t/h^2 f
20 Sept.	3.0	61.8 ± 3.6	49.7 ± 4.0	0.81	0.45				
0745 - 0850	2.9	69.6 ± 3.6	50.1 ± 2.6	0.62	0.51	69	71	1.5	0.13
	2.85	63.9 ± 3.9	47.7 ± 6.4	0.75	0.47				
20 Sept.	3.25	46.2 ± 4.3	27.4 ± 3.7	0.59	0.34				
1420 - 1500	3.25	42.5 ± 4.8	27.7 ± 6.6	0.65	0.31	45	44	7.5	0.65
	3.2	38.8 ± 3.2	27.8 ± 0.3	0.72	0.29				
20 Sept.	3.35	29.0 ± 4.0			0.21				
2120 - 2230	3.30	28.6 ± 5.2	16.5 ± 1.4	0.58	0.21	22	21	15	9.17
	3.25	34.0 ± 4.6	16.5 ± 0.5	0.49	0.25				
21 Sept.	3.3	13.5 ± 2.9	12.5 ± 3.2	0.93	0.10				
0810 - 1145	3.25	17.7 ± 1.3	10.2 ± 0.7	0.58	0.13	9	85	27	2.33
	3.25	9.85 ± 0.9	9.8 ± 1.2	0.99	0.07				
21 Sept. 1430 - 1440	3.25	16.6 ± 0.7			0.12	45	6	31.5	2.72

Exp. Period 26 - 28 Sept '81   Final ice thickness h$_f$ = 3.1 cm
Concentration 0.95%
Note: Warm-up started 27 Sept., at 0930

Date, time	Ice thickness h(cm)	Flexural strength (kPa) σ	Flexural strength (kPa) σ'	σ'/σ	σ/σ$_l$ (σ$_l$ = 66.2 kPa)	Elastic modulus (MPa) E	Elastic modulus (MPa) E'	Warm-up time t(hr)	t/h$_f^2$
27 Sept.	2.55	67.5 ± 3.6	32.3 ± 4.1	0.48					
0815 - 0940	2.5	62.4 ± 2.0	36.1 ± 4.4	0.58		79	86		
	2.45	69.7 ± 5.9	36.9 ± 4.7	0.53					
27 Sept.	2.90	39.7 ± 11.4	25.06 ± 3.2	0.66	0.60				
1315 - 1420	2.95	43.5 ± 5.6	24.7 ± 2.9	0.57	0.66	48	54	4.5	0.47
27 Sept.	2.95	21.8 ± 2.7	13.7 ± 0.0	0.63	0.33				
1800 - 1835	3.0	23.31 ± 2.3	14.5 ± 1.5	0.62	0.35		38	9.0	0.94
27 Sept. 2200	3.0	23.5 ± 1.0	10.2 ± 1.7	0.43	0.35		27	12.5	1.30
28 Sept. 0910 - 0920	3.05	24.4 ± 5.2	25.3 ± 1.2	0.74	0.35			24	2.50

Exp. Period 16 - 21 Oct '81   Final ice thickness h$_f$ = 5.0 cm
Concentration 0.95%
Note: Warm-up started 19 Oct., at 0930

Date, time	Ice thickness h(cm)	Flexural strength (kPa) σ	Flexural strength (kPa) σ'	σ'/σ	σ/σ$_l$ (σ$_l$ = 130 kPa)	Elastic modulus (MPa) E	Elastic modulus (MPa) E'	Warm-up time t(hr)	t/h$_f^2$
17 Oct.	2.00	86.9 ± 7.0	47.2 ± 6.4	0.54					
2110 - 2135	2.00	91.5 ± 21.5	45.5 ± 5.1	0.50		118			
	2.00	66.5 ± 3.2	38.5 ± 3.1	0.58					
18 Oct.	3.22 - 3.29	114.95 ± 8.3	60.4 ± 4.3	0.52					
1340 - 1430	3.24 - 3.27	99.2 ± 3.6	56.4 ± 3.1	0.57		131			
	3.31 - 3.37	106.6 ± 4.4	43.7 ± 2.2	0.41					
18 Oct. 1950	3.68 - 3.80	121.54 ± 11.	56.1 ± 4.5	0.46		122			
19 Oct. 0850	4.58 - 4.64	143.5 ± 3.3	59.4 ± 1.8	0.41		158			
19 Oct.	4.92 - 5.04	104.6 ± 8.2	48.5 ± 5.0	0.46	0.80				
1630 - 1715	4.95	96.3 ± 6.9	36.7 ± 1.0	0.38	0.74	98		3	0.12
	5.00	88.5 ± 3.2	41.0 ± 0.7	0.46	0.68				
20 Oct.	5.00	63.6 ± 7.9	20.8 ± 1.1	0.33	0.49				
0810 - 0915	5.10	52.0 ± 8.0	21.6 ± 2.6	0.41	0.40	57		18.5	0.74
	5.20	50.7 ± 5.0	18.6 ± 1.1	0.37	0.39				
20 Oct.	4.95 - 5.15	49.2 ± 3.9	18.0 ± 2.3	0.37	0.38				
1520 - 1610	5.10	46.1 ± 2.5	14.2 ± 0.9	0.31	0.36	43		25.3	1.01
	5.05	46.3 ± 8.8	10.5 ± 0.2	0.22	0.36				
20 Oct. 2300	5.00	29.8 ± 3.5	10.0 ± 0.5	0.40	0.23	25		33.0	1.32
21 Oct.	5.00	10.8 ± 1.8			0.08				
0820 - 0900	5.00	6.74 ± 1.0			0.05	11		42.5	1.70

41

Date, time	Ice thickness h(cm)	Flexural strength (kPa) σ	σ'	σ'/σ	σ/σ_i (σ_i = 135 kPa)	Elastic modulus (MPa) E	E'	Warm-up time t(hr)	t/h_f^2
13 Nov. 0800	2.1	90.8							
	2.1	76.2							
	2.3	76.7							
14 Nov. 1030	5.0	123.4							
	5.1	114.9							
	5.1	136.2							
14 Nov. 1900	5.4	94.9			0.70			6	0.19
	5.4	91.2			0.68				
15 Nov. 1100	5.4	70.6			0.52				
	5.6	69.5			0.52	64		22	0.70
	5.7	74.8			0.55				
15 Nov. 2030	5.5	71.4			0.53				
	5.6	63.8			0.47	63		31.5	1.00
	5.75	55.6			0.41				
16 Nov. 0700	5.6	18.0			0.13				
	5.6	18.5			0.14	32		42.0	1.34
	5.75	14.5			0.11				

Date, time	Ice thickness h(cm)	Flexural strength (kPa) σ	σ'	σ'/σ	σ/σ_i (σ_i = 104 kPa)	Elastic modulus (MPa) E	E'	Warm-up time t(hr)	t/h_f^2
18 Nov. 0800	2.7	87.3				62			
	2.8	101.3							
18 Nov. 0900	2.9	89.1			0.86			0.5	0.05
18 Nov. 1200	3.1	56.1			0.54				
	3.2	86.3			0.83	36		3.5	0.32
	3.1	74.0			0.71				
18 Nov. 1600	3.2	47.7			0.46				
	3.4	57.1			0.55	28		7.5	0.69
	3.3	49.4			0.48				

Date, time	Ice thickness h(cm)	Flexural strength (kPa) σ	σ'	σ'/σ	σ/σ$_i$ (σ$_i$ = 104 kPa)	Elastic modulus (MPa) E	E'	Warm-up time t(hr)	t/h^2 f
18 Nov.	3.3	30.5			0.29				
2050	3.4	39.3			0.38	19		12.5	1.15
	3.3	32.6			0.31				
19 Nov.	3.3	23.9			0.23				
0630	3.4	22.6			0.22	8		22.0	2.02
	3.3	27.0			0.26				

Exp. Period 20 - 23 Nov '81   Final ice thickness h$_f$ = 5.6 cm

Concentration 0.95%

Note: Warm-up started 21 Nov., at 0900

Date, time	Ice thickness h(cm)	Flexural strength (kPa) σ	σ'	σ'/σ	σ/σ$_i$ (σ$_i$ = 135 kPa)	Elastic modulus (MPa) E	E'	Warm-up time t(hr)	t/h^2 f
20 Nov.	2.4	84.0							
1200	2.4	90.3				66			
21 Nov.	5.0	138.8							
0830	4.8	149.1				188			
	4.6	143.1							
21 Nov.	5.6	104.3			0.77				
1730	5.6	104.9			0.78	66		8.5	0.27
	5.4	104.5			0.77				
22 Nov.	5.7	71.5			0.53				
0930	5.7	61.9			0.46	50		24.0	0.77
	5.5	54.7			0.40				
22 Nov.									
1900	5.7	30.4			0.22	41		34.0	1.08
	5.5	42.9			0.32				
23 Nov.	5.6	15.9			0.12				
0530	5.6	16.5			0.12	14		44.5	1.42
	5.5	19.5			0.14				

Exp. Period 28 Nov - 1 Dec '81   Final ice thickness h_f = 5.6 cm

Concentration 0.95%

Note: Warm-up started 29 Nov., at 1230

Date, time	Ice thickness h(cm)	Flexural strength (kPa) σ	σ'	σ'/σ	σ/σ_i (σ_i = 135 kPa)	Elastic modulus (MPa) E	E'	Warm-up time t(hr)	t/h_f^2
28 Nov.	2.1	60.6							
0900	2.1	61.0							
28 Nov.	2.9	98.5							
1800	2.9	102.4				89			
	3.0	108.1							
29 Nov.	4.8	146.7							
1100	4.8	142.0							
	4.7	150.0				183			
29 Nov.	5.4	107.1			0.79				
1800	5.4	106.1			0.79	135		5.5	0.18
	5.3	108.3			0.80				
30 Nov.	5.7	64.7			0.48				
0830	5.6	58.3			0.43	60		20.0	0.64
	5.5	61.2			0.45				
30 Nov.	5.6	62.3			0.46				
1600	5.6	59.6			0.44	60		27.5	0.88
	5.6	75.7			0.56				
30 Nov.	5.6	52.2			0.39				
2200	5.7	55.0			0.40	41		33.5	1.07
	5.5	52.0			0.39				
1 Dec.	5.6	48.3			0.36				
0530	5.7	31.5			0.23	33		41.0	1.31
	5.5	43.9			0.33				
1 Dec.									
0730	5.6	33.3			0.25	32		43.0	1.37
	5.6	30.2			0.22				

A facsimile catalog card in Library of Congress MARC
format is reproduced below.

END

FILMED

6-83

DTIC